LARGE-SCALE SYNTHESIS OF Zn_3P_2 NANOWIRES USING POROUS ZINC PELLETS

A Thesis

by

RAKESH

Submitted to the Office of Graduate and Professional Studies of
Texas A&M University
in partial fulfillment of the requirements for the degree of

MASTER OF SCIENCE

Chair of Committee,	Sreeram Vaddiraju
Committee Members,	Mustafa Akbulut
	Raghupathy Karthikeyan
Head of Department,	M. Nazmul Karim

December 2017

Major Subject: Chemical Engineering

ABSTRACT

Nanowires are nanostructures with diameters on the order of a few nanometers with an aspect ratio greater than 1000. A major challenge impeding commercialization of nanowires and nanowire-based devices is their large-scale synthesis.

Traditionally nanowires synthesized by chemical vapor deposition (CVD) are grown via the vapor-liquid-solid (VLS) mechanism using expensive catalysts, and these catalysts remain as contaminants after the synthesis. This problem can be avoided by using self-catalysis, where one of the component elements of the nanowires serves as the catalyst. Brockway *et al.* have used self-catalysis and have reported gram-scale synthesis of Zn_3P_2 nanowires using this strategy. In that work, zinc foils served as both the source and the substrate for the formation of Zn_3P_2 nanowires. However, using this method the growth of nanowires is constrained to the surfaces of the zinc foils thereby reducing the number of nanowires produced. In addition, post-synthesis nanowire collection involves brushing Zn_3P_2 nanowires out of zinc foils, which is physically difficult and time intensive.

The objective of this thesis is to convert entire zinc raw material into Zn_3P_2 nanowires in a byproduct-free manner. This has been accomplished by using Zn/NH_4Cl pellets, as pellets have better thermal transport than powdered form, leading to uniform heat distribution. In addition, in the early stages of heating, NH_4Cl sublimates leaving behind porous Zn pellets which aids the diffusion of phosphorus vapors throughout out the pellet. Thus, entire pellets are converted into Zn_3P_2 nanowires avoiding the post-

synthesis nanowire collection. X-ray diffraction analysis confirmed that resulting Zn_3P_2 nanowires were devoid of any impurities such as Zn, ZnO, $ZnCl_2$ or NH_4Cl.

ACKNOWLEDGEMENTS

I would like to express the deepest appreciation to my committee chair Dr. Sreeram Vaddiraju for his guidance and for his thoughtful inputs in technical writing. I also thank committee Dr. Mustafa Akbulut and Dr. Raghupathy karthikeyan. I also thank the Department of Chemical Engineering for providing me scholarship to fund my education.

I would like to thank my friend Yixi Chen, who has gone out of his way to help when I needed it. I also thank my colleagues: Azhar, Pranav and Venkata for making my time at the lab lot of fun. Special thanks to my friends, Yatiraj and Prashanth, for their constructive critiques throughout my work.

Finally, I would like to thank my parents for their love and support in my education. I thank my brother for being my emotional support and for believing in me.

CONTRIBUTORS AND FUNDING SOURCES

This work was supervised by a thesis committee consisting of Professor Sreeram Vaddiraju (chair), Professor Mustafa Akbulut of the Department of Chemical Engineering, and Professor Raghupathy Karthikeyan of Department of Biological and Agricultural Engineering.

This work was partially financed by Mary Kay O'Connor Process Safety Center (MKOPSC). This support was primarily used for procuring supplies necessary for performing nanowire synthesis experiments.

TABLE OF CONTENTS

Page

LIST OF FIGURES

LIST OF TABLES

CHAPTER I

INTRODUCTION

1.1 Background on nanotechnology

Nanotechnology is the science of manipulation and investigation of materials which have at least one principle dimension in the nanoscale (1nm = $1x10^{-9}$ m) [1]. Depending on the number of dimensions in nanoscale; materials are broadly classified as zero-dimensional, one-dimensional, and two-dimensional nanomaterials. Some of the zero-dimensional nanomaterials are nanoparticles [2] and quantum dots [3]. One-dimensional nanomaterials include nanorods [4], nanowires [5], nanotubes [6], and nanobelts [7]. Graphene [8] and thin films [9] are some examples for two-dimensional nanomaterials.

The concept of nanotechnology was first proposed by Richard Feynman in the year 1959 in his talk "There's plenty of room at the bottom", in which he suggested the possibility to precisely manipulate atoms or molecules [10]. However, the concept of synthesizing materials at nanoscale and utilizing the unique properties has been known for centuries even without any theoretical knowledge. Chinese pottery makers have made ruby color vases out of gold nanoparticles few hundred years ago. Historians have recently found Damascus sabre steel swords dating back to the 17^{th} century, which upon careful examination showed the presence of carbon nanotube and cementite nanowires, which resulted in their excellent mechanical strength and sharp cutting edges [11].

When the particle size reduces from macro scale to nanoscale, the number of atoms on the surface increases [12]. Hence nanomaterials are ideal candidates for surface dominant phenomena, such as adsorption and catalysis. Furthermore, nanomaterials with different particle sizes and shapes demonstrates different mechanical, optical, electrical, and thermal properties [13].

Tremendous amount of research is being done on nanotechnology to create new materials with unique properties and to develop new and improved products. In 2017, US federal budget allocated $1.4 billion for the National Nanotechnology Initiative (NNI) [12]. As a result, nanotechnology-based products have been developed or are in the process of being developed in the fields of medicine [14], electronics [15], agriculture [16], and energy [17]. In 2010, nanotechnology was estimated to represent $11 trillion of the market [18]. Revenue from nanotechnology-based products has increased by six folds from 2009 to 2016 and has been estimated to be in excess of $500 billion in 2016 [19].

1.2 Nanowires and their applications

Nanowires have a diameter in the range of 1-100 nm and an unconstrained length, usually ranging from a few to hundreds of micrometers. Among them, nanowires with small diameters (usually a few nanometers) are of great interest, because when the diameter is reduced to less than the Bohr's radius electron transport and optical properties of the materials change dramatically due to the resulting quantum confinement [20]. The corresponding unique properties could then be exploited to a wide range of commercial applications.

Nanowires have widespread applications in the fields of solar cells, memory devices, batteries, to name a few. A complete list of the applications of nanowires can be found in table 1. This is also reflected in growing interest in nanowires in the research community as shown in figure 1.

Table 1: Various possible industrial applications of nanowires

Nanowire Applications	
• Solar cells	• Processor
• Memory devices	• Chemical sensors
• OLED	• Photo detectors
• UV devices	• Li-ion Batteries
• Bio-sensors	• Nanoscale lasers
• Transparent conductive films	• Thermoelectric generators

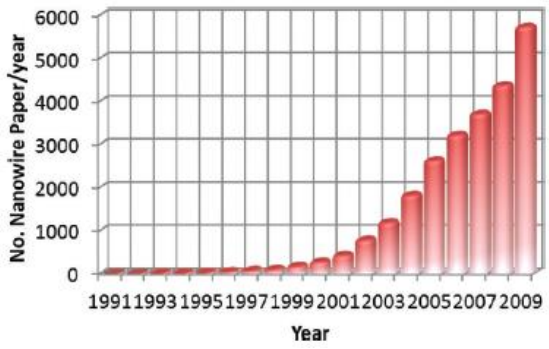

Figure 1: Graphical representation of number of nanowire related publications from 1991-2009. Plot indicates that the number of nanowire related publications have increased year over year from 1991-2009 (Reprinted from Yang *et al.*, 2010)

Nanowires are the smallest material available to transport electric charge efficiently in one-dimension. Hence, it can be used both as a wiring and a device element in nanoscale systems [21]. In solar cell applications, nanowires can be used as light absorption or as charge transport media [22]. Electron transport efficiency is higher in nanowires when compared to that in nanoparticles owing to the higher number of grain boundaries in the latter [22].

Nanowires have a high potential to replace existing bulk materials and other nanomaterials in many of the current technologies. For example, silver nanowires are considered as next generation transparent conductive electrodes in semiconductor devices. Silver nanowires alone generated revenue of $299.4M in 2016, which is estimated to grow at a compound annual growth rate (CAGR) of 6.23% and reach $408.14m by 2021 [23].

In some applications, zero-dimensional nanomaterials such as nanoparticles are considered better than nanowires, considering the formers' high potential for integration into devices and lower cost of synthesis. Taking in account available 2017 cost data [24], silver nanowires of 40 nm diameter and length of 20 microns cost $350/gm, whereas silver nanoparticles of 20-30nm diameter cost $13/gm. However, the difficulty lies in creating interconnections between the nanoparticles when scaled up [25].

1.3 Commercializing nanowire-based technology

There are three major challenges that hinder the translation of nanowires into a profitable commercial technology: mass production, stability, and assembly of nanowires. Each challenge will be briefly explained in the subsequent sections.

1.3.1 Nanowire mass production (large-scale synthesis)

To have nanowires and nanowire-based devices in the commercial market, industry must be able to produce nanowires on a large scale. The definition of 'large-scale' though varies widely from industry to lab. In industrial scale, large-scale can be defined by production of thousands of kilograms of nanowires per day whereas in lab research, the term large-scale refers to a few grams of nanowire synthesis or the ones which have potential to scale up to gram scale. The major challenges associated with scaling up a process from lab-scale to industrial-scale include [26]:

a) Synthesis is not easy to control in large reactors as number of parameters affecting nanowire growth increases.
b) Non-linear increase in raw material quantity.
c) Difficulty in controlling product quality and reproducibility.
d) Increase in cost of the reactor.

To demonstrate the need for large-scale synthesis, silicon nanowires as a potential anode material for lithium ion batteries are considered. Compared to the existing graphite anodes, the silicon based anode has a low discharge potential and the highest known theoretical capacity (4,200 $mAhg^{-1}$) [27]. As an anode material, silicon nanowires have advantages over bulk silicon. Unlike bulk silicon, silicon nanowires can withstand large volume changes during lithium insertion and extraction, which prevents cracking and pulverization of the electrode [28]. For electric vehicles, which use lithium-ion batteries of 28 KWh energy, with an active cathode material of lithium manganese oxide and

graphite as the anode, require 31 kg of graphite material to drive a distance of 161 Km [29]. Replacing graphite with silicon nanowires (with capacity 2300 $mAhg^{-1}$ [30]) as anode material will require only around 5 kg of silicon nanowires per electric vehicle. As reported in the year 2015, the number of electric cars on the road worldwide was 1.2 million, and hence, the requirement of silicon nanowires production can be estimated to be around 6000 tonnes per year [31].

1.3.2 Nanowire assembly

Nanowires are usually synthesized by two approaches, namely top-down synthesis approach and bottom-up synthesis approach. In top-down synthesis approach macrostructures or microstructures are reduced to nanowires, whereas in bottom-up synthesis approach nanowires are grown by crystallization and growth. Using the top-down nanowire synthesis approach, nanostructures can be positioned on top of another material during the fabrication stage itself, which eliminates the necessity of post-synthesis assembly of the nanowires [32]. Despite the top down approaches having an advantage of easy integration within the architecture of the device, these processes are expensive and require high labor effort. On the other hand, using bottom-up approaches nanowires of complex material system can be produced in large quantities [33] [34] [35]. However, the synthesized nanowires using bottom-up approaches are randomly oriented. Hence, assembly techniques are used to manipulate and position nanowires in the desired two-dimensional or three-dimensional format. Nanowire synthesis via bottom-up techniques followed by using assembly strategies for device fabrication has the advantage of using optimum nanowire synthesis conditions. This approach also has the added

advantage of not being material dependent and can be assembled into complex architectures.

The very idea of using nanowires as fundamental building blocks for the fabrication of next generation nano-electronic and nano-photonic devices has already been demonstrated [36] [37] [38]. Organic polymers such as polyester film is being used in current flexible electronic devices [39]. But many of these materials are not suitable for fabrication under the conventional processing conditions. Hence arrays of inorganic semiconductors could be considered for flexible electronics which exhibit high carrier mobility and excellent stability [40]. But the challenges lie in translating unique properties of nanowires in terms of optical, electrical, mechanical, and electronic properties into nanowire-based devices after assembly. In addition, nanowires should be able to retain their morphology even after the assembly.

Post-synthesis assembly techniques are broadly classified based on the applied force, for example, assembly by molecular forces [41] [42], assembly by shear force [43] [44], assembly by electrostatic interaction [45] [46], assembly within magnetic fields [47] [48], to name a few. By understanding the pros and cons of each technique and then by using a combination of these techniques, challenges associated with the assembly of nanowires can be solved. Some of the challenges with nanowire assemblies are as follows [49]:

a) High aspect ratio nanowires do not respond uniformly to the applied force.

b) Difficulty in production of highly complex assembly architectures with few defects.

1.3.3 Nanowire stability

Nanowire stability can be defined as the ability of nanowires to resist chemical change or decomposition in its natural environment. Compared to the other two challenges, there is considerably less research in the field of the nanowire stability. Stability studies are complex as the kinetics and mechanics of degradation depend on factors including shape and size of nanowire, humidity, temperature, substrate material [50]. Nanowires due to its high surface area can undergo various chemical reactions when exposed to different kinds of environment. Nanowire stability is important for the devices which need to be used for prolonged durations. For instance, devices used for *in-vitro* sensing do not demand long term stability and biocompatibility whereas for applications such as chronic *in-vivo* cell-recording, implantable devices demand long term stability [51].

The importance of the nanowire stability is explained with the example of silicon nanowires and zinc oxide nanowires. Silicon nanowires can be used in batteries [52]. At standard conditions silicon surface gets passivated reacting with oxygen to form SiO_2 [53]. SiO_2 then dissolves in the aqueous solutions by hydrolysis [54]. The passivation and dissolution process continue leading to inferior silicon nanowire property. Studies on silicon nanowire devices have shown stability only up to 3 weeks [55]. ZnO nanowires have been reported to have potential applications as biosensors [56], and lasers [57]. ZnO

dissolves in acidic conditions (4.5-5.0 pH) and in basic solutions of ammonia and sodium hydroxide (6-14 pH). Thus, it is not suitable for stable energy conversion devices without any surface protection. These two examples show how important it is to increase the stability of the nanowire materials to commercialize nanowire-based devices.

A few reports have demonstrated the use of organic molecules to passivate nanowire surfaces and increase stability [58] [59]. Organic molecules stop diffusion of oxygen or moisture to the nanowire surface. This makes nanowire surface more resistant towards oxygen and moisture assisted degradation [60]. However, the layer of organic molecule is not stable at high temperature [61]. Core-shell architecture is used to protect core nanowire material. Al_2O_3 is an example for a stable shell material [51]. It is easy to develop high quality Al_2O_3 shell on nanowire with precise thickness by atomic layer deposition technique, which showed high chemical stability [62]. Depending on the applications, more studies must be done on stability of nanowires subjected to high environmental and electrical stress [50].

1.4 Thesis outline

Large-scale synthesis of nanowires is one of the major challenges to the commercialization of nanowires and nanowire-based technology. The motivation behind this thesis is to synthesize Zn_3P_2 nanowires on a large-scale, byproduct-free manner. Different nanowire synthesis methods which have shown promise for large-scale synthesis are discussed in chapter 2. A novel substrate configuration is proposed in chapter 3, which can be used to synthesize nanowires in large scale without any post-synthesis processing.

Highly porous zinc pellets are first consolidated from a mixture of zinc flakes and ammonium chloride powder and subsequently converted to the pellets consisting of Zn_3P_2 nanowires. Preliminary experiments carried out on zinc pellets are discussed in chapter 4. An optimized experimental condition for Zn_3P_2 nanowire growth on zinc pellets is discussed in chapter 5. Conclusions drawn from this work are discussed in chapter 6.

CHAPTER II

NANOWIRE SYNTHESIS METHODS

2.1 Introduction

Nanowires are typically synthesized either by a top-down [63] [64] [65] or bottom-up approach [66] [67] [68] [69]. In a top-down approach macrostructures or microstructures are reduced to nanowires. In laboratories, advanced lithography techniques such as electron-beam writing [63], focused-ion-beam writing [64], or proximal probe patterning [65] are used for top-down nanowire synthesis. Demerits of using top-down approaches are high costs, limited choice of material systems, time intensiveness, incompatibility of surface chemistry with the tough processing condition such as corrosive etchants, high-energy radiation, and high temperature for nanofabrication [70]. On the other hand, bottom-up approaches have multiple advantages such as material diversity, cost effectiveness, scope for large-scale synthesis, multilayer nanowire synthesis [71].

Bottom-up approach nanowire growth process is essentially a crystallization process. During nanowire synthesis 1-D solid phase is evolved from liquid phase or vapor phase via nucleation and growth steps. In the nucleation step, continuous supply of building blocks (atoms or molecule) cause supersaturation in fluid phase to form aggregated clusters (nuclei) on a substrate. Nuclei acts as the seed where further addition of building blocks rearrange themselves to grow in one direction to form nanowires [72]. For nanowire growth to take place, either there should be a reversible pathway near equilibrium condition between solid phase and fluid phase (solution, vapor, melt), or

adsorbed atoms in solid phase should have high surface mobility [73]. Depending on the fluid phase, nanowire synthesis methods are broadly classified as solution-phase and vapor-phase synthesis techniques. Based on nanowire growth mechanism, bottom-up nanowire synthesis approaches are further classified as vapor-liquid-solid (VLS), vapor-solid (VS), and solution-liquid-solid (SLS), template-assisted methods. This will be discussed in detail in this chapter. Most of these techniques can produce nanowires of different shapes, compositions, and crystal structures. However, not every method can simultaneously control morphology (or shape), dimensions (length and diameter), and monodispersity (size uniformity) [72]. Over the past two decades, vast amount of research has been focused on developing new nanowire synthesis techniques. However, the thought of developing commercial devices made from nanowires using these techniques are still at an infant stage [74] [75] [76]. As a result, it is difficult to suggest which method can meet all the requirements for the large-scale production. Synthesis route (solution-phase techniques or vapor-phase techniques) should be chosen based on the requirement of nanowires in the most readily usable form in the devices. For example, silver nanowires can be used to replace indium-tin oxide based transparent conducting films; owing to the formers' better mechanical and electronic performance [77] [78]along with its lower cost [79]. Silver nanowire based films can be fabricated by spin coating or spray deposition from the nanowire solution. Since the raw material for conducting films are required in solution phase, it is better to adopt solution based nanowire synthesis method for this application. Synthesis methods which have shown potential for large-scale nanowire production are discussed in this chapter.

2.2 Solution-phase synthesis

Solution-phase synthesis is a common approach to produce varied nanowire systems. In general, solution-phase synthesis techniques have numerous advantages over the vapor-phase synthesis techniques. Some of the benefits of using solution-phase synthesis techniques include low costs, low temperature, and easiness in controlling the composition [80].

Various research groups have demonstrated large-scale synthesis of nanowires using solution-phase synthesis methods such as hydrothermal/solvothermal method [66] [81], solution-phase catalyst-assisted synthesis method [67], and electroless etching method [82]. One of the flowing nanowire growth mechanisms can be used to synthesize nanowires:

a) Growth from intrinsically anisotropic crystal structure.
b) Seed mediated growth.
c) Kinetic control caused by capping agent.
d) One-dimensional oriented deposition.
e) Chemical transformation of one-dimensional templates.

The underlying concepts of nanowire growth mechanism are not well understood in solution-phase techniques. Without strong fundamental knowledge, it is difficult to extend these techniques to broad material system. This also leads to the difficulty in controlling properties such as composition, shape, and size of nanowires [80].

2.2.1 Hydrothermal/solvothermal method

Hydrothermal/solvothermal method is defined as: “any heterogeneous or homogeneous chemical reaction in the presence of a solvent (aqueous or non-aqueous) above room temperature and at a pressure greater than one atmosphere in a closed system” [83]. Only difference between hydrothermal and solvothermal methods is that the latter uses solvent other than water. In a typical experiment, a solution is placed in an autoclave at temperatures between 100 °C and 300 °C and at pressure higher than atmospheric for around 24 hours. An autoclave has two zones: the hotter zone, where dissolution takes place and the cooler zone, where seed growth takes place [22]. This method, sometimes also called solution-solid (SS) method, usually involves no catalyst. Nanowires can also be synthesized using a substrate coated with seeds [81]. Ag [66] and Cu [84] are synthesized in a large-scale via this synthesis method. Often nanowires synthesized by this method are found to have poor yield, low purity (mixture of different nanostructures), and poor uniformity in size and shape. Most importantly, the underlying principle for 1-D growth is not fully understood [80]. Concentration of reactants and pH values of the solution are known to play important roles in the size and the shape of nanowires [22].

High anisotropic bonding in crystal structure results in 1-D nanowire growth. For example, trigonal selenium (t-Se) nanowires were synthesized in large quantities. In the first step, selenious acid is reduced to monodispersed spherical colloids of amorphous selenium (a-Se) at a temperature around 100 °C in the presence of excess hydrazine. These spherical colloids of a-Se aggregate in solution and then split into irregular colloids. Upon cooling to the room temperature, some of the solid Selenium dissolved in the solution

precipitate out as nanocrystallites of t-Se. During the ageing step, mass transfer of atoms takes place from high free energy a-Se to the seed t-Se to form Se nanowires [85].

In the hydrothermal method, the use of appropriate surfactants or capping agents is important to stabilize the solution system. This helps in producing high-quality nanowires, because these materials will passivate (prevents oxidation and aggregation) on the surface of growing crystals and thus reduce their surface energy [86]. Polyol reduction synthesis method is used for the synthesis of metal nanowires, e.g., Cu [87], Pt [88], and Au [89] nanowires, where a surface capping agent is used to direct 1-D growth. Common chemicals used in polyol reduction method are, ethylene glycol (EG) which acts both as a reducing agent and also as a solvent, polyvinylpyrrolidone (PVP) as capping agent, $AgNO_3$ as precursor, and chloride salts as control agent. Gram-scale synthesis of Ag nanowires using polyol reduction method have been reported in the literature [90] [91] [92].

2.2.2 Catalyst-assisted solution-phase synthesis method

Metal and semiconducting nanowires can also be synthesized with the assistance of a catalytic material in a solution. In catalyst-assisted solution-phase synthesis method, catalytic liquid droplets form in a solution and promote anisotropic growth of nanowires. Accordingly, it is also called a solution-liquid-solid (SLS) growth synthesis method.

Solution-liquid-solid (SLS) growth mechanism

In the mid-1990s, Buhro *et al.* synthesized InP, InAs, and GaAs nanowires using a simple, low temperature, solution phase reaction [93], which led to the inception of

nanowires synthesis using SLS principle. Figure 2 shows schematic representation of nanowire formation via SLS growth mechanism. In general, reactive metalorganic precursors and a nano-metal catalyst are added to the organic solution. Typically at temperatures of 200-350 °C, a low melting point catalyst melts to form a droplet. Catalyst droplets hasten the decomposition of precursor which then dissolves into the catalyst droplet. Above supersaturation point, decomposed material separates out as nanowires [80]. Nanoparticles made of low melting metals such as In, Sn, Ga, and Bi have proved to be useful for semiconductor nanowire synthesis by SLS method. Although high melting nanoparticles such as Au are readily available, their size must be limited to 1-3 nm to keep melting point of Au within the boiling point of organic solvents [94]. In a slightly different method to SLS method, called the supercritical fluid-liquid-solid (SFLS) growth mechanism larger Au nanoparticles are used under super critical solvent conditions. For example, silicon nanowires are synthesized by dissolving diphenyl silane and Au catalyst in supercritical hexane at 500°C and around 250 bar pressure. Diphenyl silane decomposes and dissolves in the gold catalyst droplets to form silicon nanowires [67].

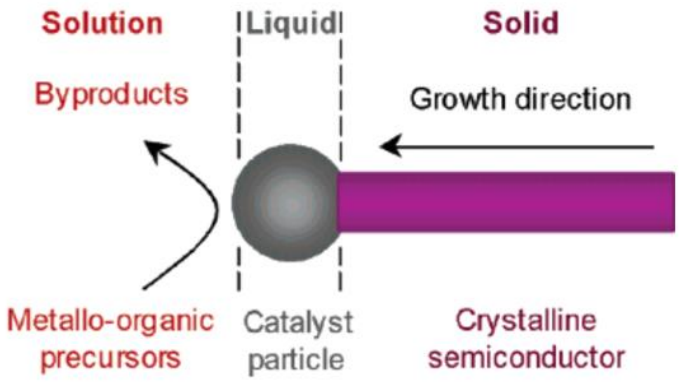

Figure 2: Illustration of SLS growth mechanism (Reprinted from Wang *et al.*, 2016)

Melting point, semiconductor-component solubility, and reactivity are some of the important criteria that are used to select catalyst materials [94]. Catalyst materials must be molten at the reaction conditions. Semiconductor component should have limited solubility in the catalyst droplets, so that high supersaturation could be achieved. Lastly, catalyst material should not react with target semiconductor phase as it can reduce the quality of the final product [95]. Compared to the VLS method for nanowire synthesis, nanowires grown by SLS typically have smaller diameter (4-10 nm). This leads to a more significant blueshift due to a stronger quantum confinement effect [96], and the length of nanowires grown by SLS is shorter (1-100 um) than that by VLS (10-1000 um). Furthermore, like other solution-phase synthesis methods, kinetics of a SLS growth can be controlled via surfactants, surface coordinating ligands, or capping reagents. This also allows for tuning the dimensions, surface structures, and morphology, as well as the electrical, thermal, and optical properties of nanowire [95].

2.2.3 Electroless etching method

Silicon nanowires are synthesized in a wafer scale through electroless etching method [82] [97]. This method has several advantages over other silicon nanowire synthesis techniques, which include:

a) Mild temperature.

b) No vacuum requirement.

c) Large scale synthesis.

d) Low cost equipment.

e) Highly aligned silicon nanowires.

In this method silver is introduced to the solution containing HF as $AgNO_3$ [97] [98], or Ag is directly deposited onto a silicon wafer. The growth mechanism is based on Ag induced selective etching of silicon as shown in the figure 3. Ag ions get reduced as per the reaction $Ag^{+}+e^{-}\rightarrow Ag_{(solid)}$. This results in the formation of Ag nanoparticles on the silicon surface. Ag nanoparticle acts as cathode and silicon surface beneath it acts as active anode. Silicon surface beneath Ag nanoparticles undergo local oxidation as per the reaction $Si_{(solid)}+2H_2O-4e^{-}\rightarrow SiO_{2(solid)}+4H^{+}$ and gets etched by HF forming pits. Continuous redox reaction increases pit depth to form silicon nanowires [82].

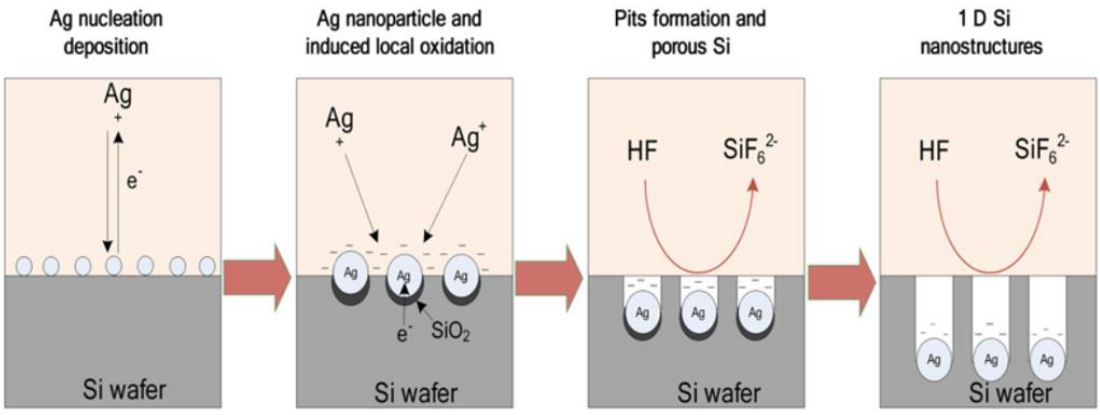

Figure 3: Silicon nanowire growth mechanism by Ag induced chemical etching of silicon surface in HF-AgNO3 solution (Reprinted from Zhang *et al.*, 2014)

2.3 Vapor-phase synthesis

Growth of nanowires is relatively simple when the solid material is an anisotropic crystal. In isotropic crystal, symmetry must be broken during nucleation step to grow 1-D nanowires [99]. Previously, it was shown how capping agents and surfactants assist in the 1-D growth of nanowires in the solution phase [89]. In vapor-phase synthesis route, either templates are used to direct 1-D nanowire growth, or in vapor-liquid-solid (VLS) based growth mechanism, symmetry is broken by flat solid-liquid interface [100]. Degree of supersaturation is a critical factor in determining the morphology of the final product. Nanowire growth takes place at relatively low supersaturation levels. Medium supersaturation leads to bulk crystals whereas powders are formed at high supersaturation level. Apart from degree of supersaturation, nucleation size and growth time determines the thickness of the nanowires [72].

Vapor-phase synthesis techniques are commonly used to synthesize nanowires of many material systems [101] [102] [103]. Most of the vapor-phase nanowire synthesis equipment are costly due to the requirement of vacuum system. It is hard to control the dimension and uniformity of nanowires due to the involvement of multiple complex phenomena (vapor transport, thermodynamics, kinetics, surface chemistry, etc.). However, most of these techniques do not require templates. Hence, it reduces time (post processing time to remove templates, time required for cleaning the templates), has better surface quality of nanowires, and less impurity [22]. Generally, these methods are easy to scale up and are also time efficient. Hence, they are promising routes for large-scale production. Various nanowires are synthesized in a large quantity using physical vapor deposition (PVD) [104] [105] [106] [107], chemical vapor deposition (CVD) method [68] [69] [108], and carbothermal reduction method [109] [110] [101].

2.3.1 Physical vapor deposition method

Experimental setup for physical vapor deposition (PVD) method consists of a tube furnace with two or three heating zones, source materials loaded in alumina crucibles, and a substrate material as shown in the figure 4. The source is kept at the hot end of the reactor. A carrier gas is used to transport evaporated source materials from the hotter end to the cooler end. At the cooler end, vapor condenses onto the substrate to form nanowires [22].

Nanowire growth mechanism through PVD is commonly known as vapor-solid (VS) growth mechanism. Critical factors influencing nanowire growth in PVD technique

are degree of supersaturation and surface energy of growing surface planes. Degree of supersaturation determines the growth rate of the crystal whereas surface energy of the growing surface determines growth of which planes are preferred. Nanowire growth in the PVD reactor is influenced by factors such as temperature, diameter of the furnace, heating rate, gas flow rate, and the distance between source and substrate material [104]. TiO_2 [105] [111], ZnO [112] [106] [107], SnO_2 [102], and other metal oxide nanowires are synthesized using this method.

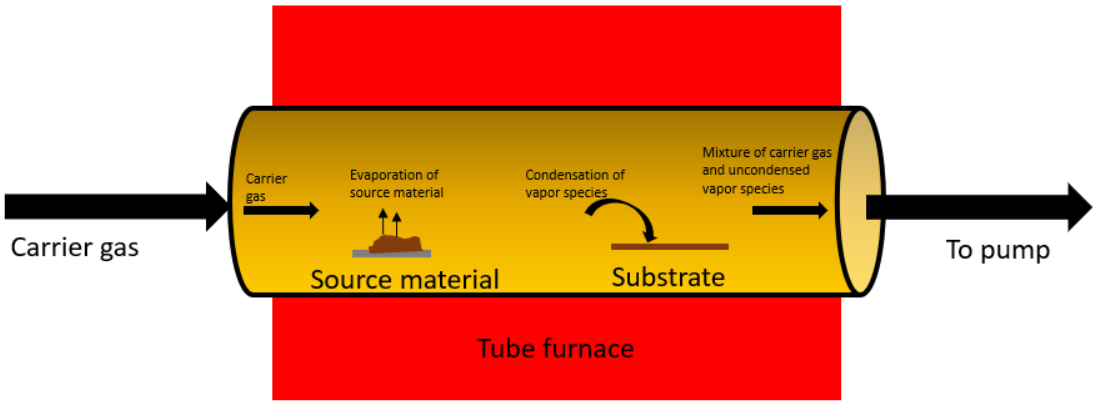

Figure 4: A typical experimental setup for nanowire growth via PVD

Vapor-Solid (VS) Growth Mechanism

VS process is also referred to as evaporation-condensation process. The driving force for spontaneous nanowire growth in VS growth mechanism is a decrease in Gibbs free energy. Decrease in Gibbs free energy is achieved by condensation of a species from supersaturated vapor. The formation of nanowires is due to anisotropic growth which can be explained by one of three mechanisms [113]:

a) Different growth rates for different facets in a crystal, e.g. {110} facets have faster growth rate compared to {111} facets for silicon diamond structure.
b) Due to screw dislocation.
c) Poisoning by impurities on specific facets.

Initially, growth species diffuses from a vapor phase to the growing surface. This is followed by adsorption/desorption onto or from the surface. Further, this species diffuses to nucleation sites, resulting in nucleation on the surface. When the concentration of the species is high, crystal growth takes place to form nanowires. Adsorption or anisotropic growth is the rate determining step [113].

2.3.2 Chemical vapor deposition method

Chemical vapor deposition (CVD) is a common method to synthesize elemental, binary, and compound semiconducting nanowires in a large quantity. Its overall process is similar to that of PVD, but the main difference is that in the case of CVD, various chemical reactions such as thermal decomposition, reduction, oxidation, disproportionation, or compound formation can take place inside the reactor [113]. As the reaction involves parallel unwanted reactions, byproducts need to be taken care of during the synthesis process itself. Experimental setup is like PVD, but in the case of CVD catalyst particles are either coated on the substrate or formed in-situ inside a reactor during synthesis. Catalyst melts and forms liquid droplets on a substrate at synthesis temperatures which dissolves the incoming vapor to form nanowires. This mechanism is referred to as the vapor-liquid-solid (VLS) growth mechanism. In some cases, low melting metal

clusters act as catalyst for 1-D growth of their compound materials as nanowires. This technique of nanowire synthesis that uses no foreign catalyst is called as self-catalysis [68] [69] [108]. In the self-catalysis, metal must be molten at synthesis temperature and gas-phase must be sufficiently reactive so that gas phase selectively reacts with metal clusters compared to bare substrates [22]. In the former case, at the end of the experiment, catalyst can be seen at the tip of grown nanowires. Parameters such as gas flow rate, source composition, type of catalyst, and temperature of different zones of the reactor determine the chemical composition and morphology of the nanowires [114]. These methods can produce a large quantity of nanowires in a short span of time and does not require large reactors [108]. Furthermore, the final product is readily usable for dry applications such as nanowire electrodes [115], solar cells [116]. Also, nanowires of high melting point material can be synthesized [115]. This method is also favorable for producing nanowires of unique properties using various dopants and can be easily integrated with other advanced technology (Thin films technology) [117].

Vapor-liquid-solid (VLS) Growth Mechanism

Amongst all the vapor based synthesis methods, VLS mechanism is the most widely studied. The advantage of using this method is that large quantities of single crystalline nanowires can be successfully synthesized [100]. In the early 1960's, Wagner and Ellis first proposed this method to synthesize micrometer scale whiskers [118]. Later, in 1998, Lieber *et al.* used a laser ablation method to produce nanometer size catalyst clusters to synthesize bulk quantities of single crystal Si and Ge nanowires [119]. Yang and co-workers studied Ge nanowires growth using GeI_2 vapor source and Au catalyst in

an in-situ high temperature transmission electron microscope (TEM). Experimental results confirm that three stages exist in VLS mechanism, they are [120]:

a) Metal alloying.

b) Crystal nucleation.

c) Axial growth.

Three stages of VLS mechanism is explained in detail using figure 5. Initially, the source material in the vapor phase gets absorbed into the molten catalyst droplet. Continuous dissolution from the gas phase leads to the supersaturation of the solute in a liquid alloy, leading to nucleation event which generates a solid precipitate of the source material. These nuclei act as preferred sites for further deposition of the material promoting tip lead growth to form nanowires. This prevents nucleation of another seed on the same catalyst droplet. Diameter of the nanowires thus produced are dictated by the catalyst droplet size. The catalyst droplet catalyzes the dissolution of vapor species, and therefore growth rate is faster in VLS mechanism compared to VS mechanism. The quality of the nanowires produced by this method is compromised by the presence of catalyst material on the tip of the grown nanowires [86]. But in the case of self-catalysis scheme, since substrate itself acts as the catalyst, it avoids foreign catalyst impurities in the final nanowire product. For example, Brockway *et al.* synthesized Zn_3P_2 nanowires in a CVD chamber using zinc foils as the substrate and catalyst. It is theorized that initially zinc foil reacts with the phosphorus to form zinc phosphide crystal nuclei. Then, the zinc adatoms diffuse to form zinc droplets on the top of crystal nuclei. These zinc adatoms could either come from the condensation of vaporized zinc or from surface diffusion of zinc from the

foil. Next, Zinc droplets formed act as a catalyst and dissolve phosphorus vapors. Lastly, in the zinc droplets zinc reacts with phosphorus to form zinc phosphide. Supersaturation of zinc phosphide in the zinc droplets leads to 1-D epitaxial growth of zinc phosphide nanowires [108].

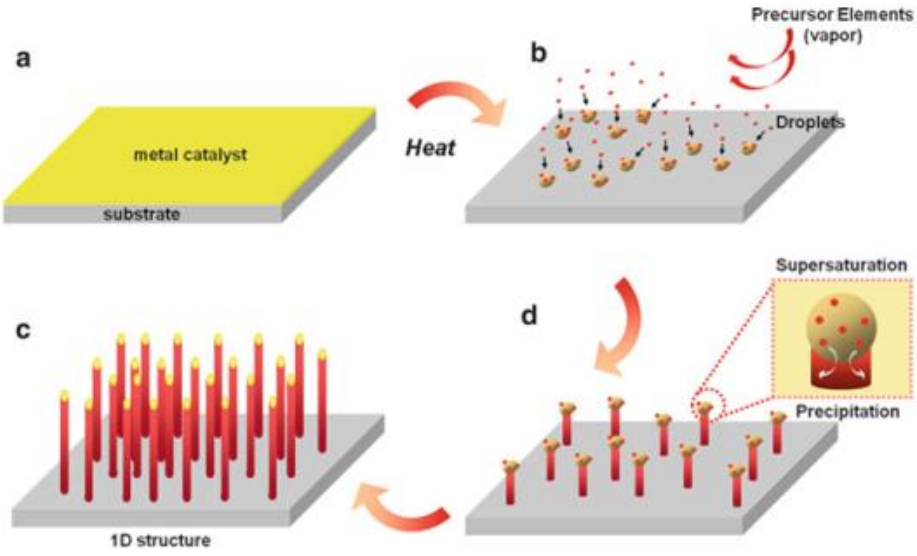

Figure 5: Schematic diagram illustrating VLS growth mechanism of nanowires (Reprinted from Choi, 2012)

2.3.3 Carbothermal reduction method

Carbothermal reduction method is the process of heating oxide precursor along with carbon to produce sub oxide vapor species. Sub oxide vapor species reacts with C, O_2, N_2, or NH_3 to form carbides, oxides, or nitrides [121]. The experimental setup for carbothermal reduction method is like that of PVD. Growth mechanism can be either VS

or VLS. For example, mixture of Ga_2O_3 and carbon when heated in an NH_3 atmosphere, bulk quantities of GaN nanowires were formed [122]. Reactions involved are:

$2Ga_2O_3 + 3C \rightarrow 2Ga_2O + 3CO_2$

$Ga_2O + 2NH_3 \rightarrow 2GaN + 4H_2 + H_2O$

In carbothermal reduction method, the two reaction steps during synthesis maintain the supersaturation of the system at a relatively low level. By controlling the supersaturation at a relatively low level, it is possible to process any solid material into nanowires [72]. Many researchers have reported large scale synthesis of SiC nanowires using this method [109] [110] [101]. Also, Banerjee *et al.* have synthesized grams of ZnO nanowires using carbothermal reduction method [123].

2.4 Template-assisted synthesis

Nanowires can be synthesized using templates. There are two different approaches for template-assisted synthesis to produce nanowires. The first method is known as the template-directed nanowire synthesis technique. In this method, nanowires are synthesized either inside the pores of the template (negative template based) or around the template (positive template based) [22]. The common negative templates are anodized alumina membrane (AAM) [124], polycarbonate membrane (PCM) [125], and mesoporous silica [98]. Carbon nanotube (CNT) is an example of a common positive template [126]. Various methods are used to deposit material onto the templates. A few research groups have reported electrochemical deposition as a promising method for nanowire synthesis in a large scale [127] [128]. The second method is known as the

chemical conversion of 1-D sacrificial template. In this method, nanowires are synthesized either by a solution-phase or a vapor-phase synthesis method. Then the nanowires are reacted with a chemical to convert them to desired compound nanowires.

Template-assisted synthesis methods give better control over the dimension and the uniformity of nanowires when compared to the nanowires produced by the techniques that have been discussed in sections 2.2 and 2.3. Demerits of template-based synthesis techniques are polycrystalline nature of resulting nanowires, difficulty in selecting appropriate template that have optimum number of pores of desired pore length and diameter. Templates should also be compatible at reaction conditions and environment. Finally, post-synthesis process involves removal of template which can compromise integrity of the synthesized nanowires [129].

2.4.1 Electrochemical deposition

Electrochemical deposition (also known as electrodeposition) has been used to grow thin film on conducting surfaces. Thin films grow normal to the conducting surface. The same principle can be used for nanowire growth by depositing on the pores of the template [86]. In general, electrodeposition can also be performed without templates, but the growth of nanowires becomes random and difficult to control. Templates with desired number of pores can facilitate nanowires to grow in a controlled manner. The typical experimental set up consists of three electrodes: working electrode (cathode), counter electrode (anode), and reference electrode. Cathode is connected to the negative terminal of the battery, whereas anode is connected to the positive terminal. Electrodes are

immersed in an electrolyte solution which contains metal ions. When electricity flows through the circuit, metal ions move towards the cathode which consists of pre-fabricated template, and deposits from the base of the electrode [22]. Upon initial deposition of the material, current must pass through the deposit for further deposition process to continue and to form nanowires. In general, this synthesis technique is applicable to electrical conductive materials such as metals, alloys, semiconductors, and electrically conductive polymers and oxides.

One of the critical factors that control the morphology of one-dimensional nanostructures by electrodeposition is the relative strength of adhesion between the depositing materials and template wall surfaces [129]. Hollow nanotubes will be produced if the adhesion between depositing materials and the wall is strong, in which case, the deposition starts from the inner walls of pores and continues inwardly. If nanowires are preferred, adhesion between depositing material and wall should be weak, in which case, the deposition starts from bottom of the template (conductive base) and continues along the pore. Other factors to be considered are applied potential, temperature, and electrolyte concentration.

Advantages of electrodeposition nanowire synthesis methods are as follows:

a) Low temperature operation.
b) Low Cost.
c) Ability to synthesize striped nanowires, i.e., nanowires with multiple segments of different metals.

d) Ability to control the aspect ratio of nanowires by controlling various parameters (applied potential, concentration) or length and diameter of template pores.

Disadvantages of electrochemical deposition nanowire synthesis methods are [22]:

a) If pore diameter is too small, deposition becomes harder due to pore clogging and slow diffusion transport.
b) When pores are filled with material, deposition process must be stopped or else a continuous film will be formed on the top of the template.
c) Limited substrate material choice due to the requirement of conductive material. This is applicable mainly for metallic nanowire synthesis as metal ions have to migrate in the presence of applied electric field.
d) The template removal process is time intensive and reduces the surface quality of nanowires. Templates may also result in polycrystalline nanowires.

2.4.2 Chemical conversion of 1-D sacrificial templates

Chemical conversion of 1-D sacrificial template method uses previously synthesized nanowires as a consumable nanowire templates. In this technique, nanowires are initially synthesized and then reacted with different chemicals to form desired final product. Even though, the synthesized nanowires have poor alignment, this technique is favorable to synthesize nanowires of numerous material systems at a low temperature in large quantities [129].

As discussed in section 2.2.1, the intrinsic anisotropic nature of trigonal phase Se and Te can be used to synthesize nanowires of Se and Te, respectively, in the solution

phase in large quantities [85]. Some examples of using intrinsic anisotropic materials as a sacrificial template are mentioned here. Gates *et al.* chemically transformed t-Se nanowires to Ag_2Se nanowires via topotactic reaction by adding Ag^+ to an aqueous solution containing t-Se nanowires [130]. Jeong *et al.* synthesized single crystal Ag_2Se and then transformed to CdSe nanowires via cation exchange reaction [131] [132]. Scott *et al.* demonstrated gram-scale synthesis of Bi_2Te_3 and PbTe nanowires using Te nanowires as templates and then chemically converting it by adding appropriate cation precursors to the solution [133]. Kang *et al.* synthesized Mg_2Si nanowires by reacting Mg vapors with silicon nanowires template [134].

Challenges involved in using nanowires as templates are the difficulty in controlling the composition and crystallinity of the final product. This is due to the limited understanding of reactions on template at the atomic scale. Until now, very few single crystalline semiconductor nanowires have been synthesized by the sacrificial template method [72].

Nanowires of many desired material systems can now be synthesized in large quantities by vapor-phase and solution-phase synthesis methods [135]. In this chapter, pros and cons of each synthesis method have been discussed. Time is an important factor to be considered for industrial scale-up [26]. Amongst different nanowire synthesis methods that are discussed in this chapter, CVD requires shorter synthesis time as shown in figure 6. However, a nanowire synthesis method must be chosen based on the requirement of the material system. For example, silver nanowires are produced in wafer-scale through solution-phase route [82]. Hence, it is economical for industry to adopt

solution-phase synthesis method to produce silver nanowires. Plasma-based methods have very short synthesis time. However, these methods have not been discussed in this chapter due to their limitations such as [26]:

a) Only metal oxides have been synthesized in a large-scale.

b) Unavailability of a theory that explains nanowire growth.

c) Limited understanding of role of plasma parameters on nanowire growth.

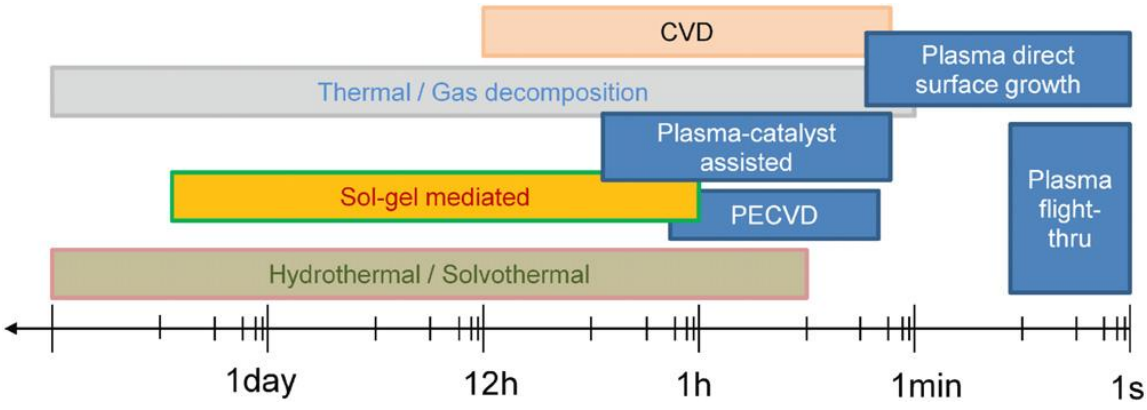

Figure 6: The graph indicates the synthesis time for different nanowire synthesis methods. This shows that the synthesis time required for CVD is less than the time requirement for other popular nanowire synthesis techniques (Reprinted from Cvelbar, 2011)

So far, many binary semiconductor nanowires have been synthesized using CVD [108] [136] [137] [138] [139] [140]. In the following chapter, various research publications on Zn_3P_2 nanowire synthesis methods are briefly discussed. In addition, a novel method for the large-scale nanowire synthesis of Zn_3P_2 has been put forward.

CHAPTER III

PROBLEM STATEMENT AND HYPOTHESIS

3.1 Zinc phosphide (Zn_3P_2) nanowires

Zn_3P_2 has a face centered cubic (FCC) tetragonal crystal structure, with lattice parameters a = b = 8.0889 Å, c = 11.4069 Å [141]. A unit cell of Zn_3P_2 consists of 40 atoms (24 Zn atoms and 16 P atoms) as shown in figure 7. Its crystal structure is described as distorted anti-flourite structure, where zinc atoms occupy only three quarters of voids formed by phosphorus tetrahedra. Unoccupied voids are highlighted in green in figure 7 [142]. Zn_3P_2, with band gap of 1.5 eV, large optical absorption coefficient ($<10^4$ cm^{-1}), and long minority carrier diffusion length of around 13 μm is a promising material for photovoltaic applications [143]. Studies on Zn_3P_2 indicate low lattice thermal conductivity [142]. Hence, it is also considered as promising thermoelectric material. It is reported that bulk assembled Zn_3P_2 nanowires show decreased thermal conductivity and increased electrical conductivity over bulk Zn_3P_2 [144].

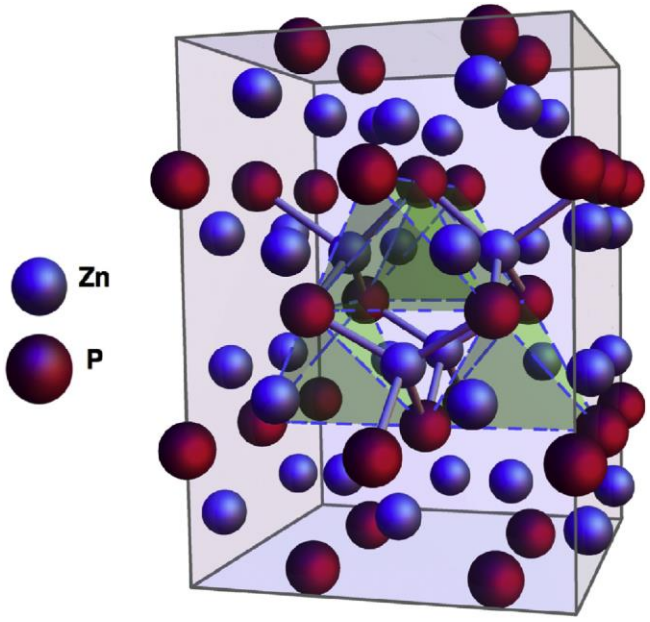

Figure 7: Tetragonal crystal structure of Zn_3P_2. The unit cell of Zn_3P_2 crystal consists of 24 zinc atoms (indicated by blue spheres) and 16 phosphorous atoms (indicated by red spheres) (Reprinted from Thompson *et al.*, 2016)

Zn_3P_2 nanowires have been synthesized mainly by vapor-phase synthesis methods. Some of the noteworthy research in this field include, synthesis of Zn_3P_2 nanowires in a CVD chamber using Zinc powder and InP powder as source material, and gold film as the catalyst [145]. Wu *et al.* produced single crystalline Zn_3P_2 nanowires via a facile catalyst-free physical evaporation process using Zinc grains and InP powders [143]. Vasekar *et al.* used chemical reflux method to synthesize Zn_3P_2 nanowires using zinc foil and trioctylphosphine [146]. Kamimura *et al.* reported 50-200 nm Zn_3P_2 nanowires synthesized based on VLS growth method [147]. In addition, core-shell architecture of Zn_3P_2 nanowires [148], hierarchical tree-shaped nanowires have been synthesized [149]

As far as large-scale synthesis of Zn_3P_2 nanowires is concerned, only Brockway *et al.* have synthesized 250 mg of Zn_3P_2 nanowires in a span of 45 minutes, via a direct reaction of zinc roll and red phosphorus in a CVD chamber [108]. Although nanowires can be synthesized in large-scale in a short span of time, synthesized nanowires must be brushed off from the zinc foil. This post-synthesis processing takes around 1 hour. The extension of this work is to use an alternative zinc material which could entirely convert into Zn_3P_2 nanowires. This could eliminate the challenges in post-synthesis processing. The hypothesis of this work is outlined in the following section.

3.2 Hypothesis

Large-scale synthesis of Zn_3P_2 nanowires could be accomplished using porous zinc pellets in a chemical vapor deposition (CVD) chamber. Generally, Zn_3P_2 nanowires are synthesized using zinc foils or zinc powders as substrate. The randomly distributed zinc powders at substrate region will be heated non-uniformly and any spatial variation in temperature will result in very low yield and non-uniform nanowires. In addition, powder distribution will not be same for each synthesis trial hence, it would be hard to reproduce the results. On the other hand, nanowires synthesized in zinc foils will require longer nanowire removal time. To overcome these problems, it is proposed that nanowires could be synthesized using zinc pellets. Consolidation of zinc powders into a zinc pellet is expected to increase the thermal transport due to the high surface contact between each zinc powder and decrease the spatial temperature variation. This would result in uniform distribution of nanowires and a higher yield. However, zinc pellets could produce nanowires only on the surface of the pellet due to no direct contact between the inner

region of the pellet and the vapor species (phosphorus vapor). To overcome this problem, it is proposed to use porous zinc pellets could be used as the starting material. It is the hypothesis of this work that pellets made by consolidating mixture of zinc flakes and salt (NH_4Cl) with a low sublimation point could be used to produce porous zinc pellets. At synthesis temperature salt is expected to sublime leaving behind high porous zinc pellet. Pores in the pellet would prevent zinc particles from coalescing into one particle, and would aid the phosphorus vapors to diffuse to the inner region of the pellet to form Zn_3P_2 nanowires on the entire pellet. Hence the post-synthesis processing could be avoided and large-scale, byproduct-free Zn_3P_2 nanowire synthesis could be accomplished.

The objective of this thesis is to convert entire zinc/NH_4Cl mixture pellets into Zn_3P_2 nanowires in a large-scale, byproduct-free manner.

CHAPTER IV

PRIMARY STUDIES ON ZINC PELLETS

4.1 Overview

In this chapter, the parameters affecting nanowire growth have been comprehensively discussed. Experimental observations and conclusions drawn from this chapter have aided in optimizing the nanowire yield as discussed in the subsequent chapter.

Brockway *et al.* [108] showed that Zn_3P_2 nanowires could be synthesized in large quantities using phosphorus vapor transport onto heated zinc foils. But the zinc substrate conversion was low. Percentage yield of Zn_3P_2 nanowires per gram zinc metal basis ($\frac{\text{grams of the synthesized } Zn_3P_2 \text{ nanowires}}{\text{grams of zinc raw material}}$ x 100) is calculated to be approximately 1.56%. Hence to improve Zn_3P_2 nanowire yield, in this thesis, zinc/NH_4Cl mixture pellets were used and experimental parameters were individually tuned to optimize the results.

4.2 Materials and methods

4.2.1 Materials

Zinc flakes (325 mesh, 97% metals basis) – Alfa Aesar, phosphorus powder (100 mesh, 98.9% metals basis) – Alfa Aesar, ammonium chloride (ACS Grade) – Amresco, zinc foil (0.25mm thick, 30 cm wide, 99.98% metals basis) – Alfa Aesar, hydrogen gas (99.999% pure) – Praxair, microscope glass slides (CAT.NO. 7101) – Alibaba, quartz tube - Chemglass, porcelain crucible (100 mm length, 20 mm width, 13 mm height) – VWR International.

4.2.2 Methods

Preparation of Zinc Pellets

Zinc flakes and NH_4Cl powders were mixed and ground using mortar and pestle at different weight ratios. The powder mixture was then consolidated into pellets by uniaxial pressing at a pressure of 76 MPa. Resulting pellets were 1 cm in diameter and 5 mm in thickness.

Synthesis of Zn_3P_2 Nanowires via Chemical Vapor Deposition

Zn/NH_4Cl mixture pellets are converted to zinc phosphide nanowires using reactive vapor transport in a hot walled chemical vapor deposition chamber (CVD) as shown in the figure 8 (b).

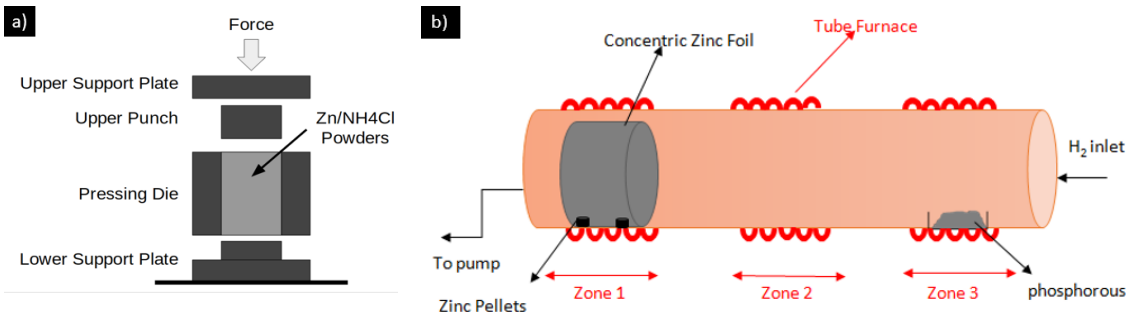

Figure 8: (a) A schematic illustrating die pressing and pellet fabrication. (b) A schematic illustrating the CVD setup used for primary studies of Zn_3P_2 nanowire growth on zinc pellets.

The CVD reactor comprises of a 1.5-inch diameter quartz tube which acts as a reactor chamber, housed within the oven (Thermo Scientific Lindberg/Blue M) that serves

as the heating source. Three different zones of the oven can be independently set to various temperatures. Inlet of the quartz tube is connected to mass flow controllers, while the outlet is connected to a pressure transducer and a pump. Pressure inside the quartz tube is maintained at around 200-700 mTorr. Substrate is placed in the zone 1 (downstream) and the source i.e., red phosphorus is placed in the zone 3 (upstream) of the reactor. In the first set of experiments, zinc foil of dimensions 15cm x 6cm was dipped in 1M HCl solution for five minutes to remove the native zinc oxide layer. Zinc foils are then rolled concentrically to form a 1.5-inch diameter coil. Two zinc pellets comprising 1:1 weight ratio of zinc to ammonium chloride were kept at the two ends of the zinc foil. They were then placed in the zone 1 of the reactor as shown in the figure 8 (b). Previous experimental conditions from Brockway *et al.* [108] as mentioned in table 2 were used to compare the nanowire growth on the zinc foil and zinc pellets. In the second set of experiments, to study the effects of various parameters on nanowire growth the following parameters were tuned: zone 1 temperature, hydrogen flowrate, preheating time of phosphorus and zinc, reaction time, and zinc to ammonium chloride ratio. In the final set of experiments, zinc pellets were placed on microscope glass slides of thickness 1mm-1.2mm, width and length 1" and 3" respectively. The morphology of the final product was characterized using scanning electron microscopy (JEOL JSM 6460).

4.3 Results and discussion

4.3.1 Imitation of previous experiment

Experiments were carried out in the CVD reactor using experimental set up and conditions similar to that demonstrated by Brockway *et al.* [108]. 500 mg of two zinc

pellets made by mixing 1:1 weight ratio of zinc flakes and ammonium chloride powders were placed at the two ends of the zinc foil as shown in the figure 8 (b). The experimental conditions are mentioned in the table 2.

Table 2: Conditions used by Brockway *et al.* for Zn_3P_2 nanowire synthesis on the zinc foil [108]

Parameters	**Zone 1**	**Zone 2**	**Zone 3**
Temperature [°C]	400	400	485
Preheating time [minutes]	5	5	10
Reaction time [minutes]	40	40	35
Phosphorous quantity [mg]			300
Hydrogen flow rate [sccm]	20		

Zinc foil as a substrate material along with similar experimental conditions to that of previous work was used as a starting point for two reasons:

(i) Brockway *et al.* were able to synthesize Zn_3P_2 nanowires on the entire surface of the zinc foil. The ratio of amount of zinc in the foil to that in pellets is 64:1. The amount of zinc in the pellet is very small compared to that in the foil.

Therefore, using both zinc foil and zinc pellet as substrate material is expected to produce Zn_3P_2 nanowires both on the foil and pellets.

(ii) Zn_3P_2 nanowire growth on the zinc foil takes place as per the self-catalysis growth mechanism explained in section 2.3.2. Similarly, for zinc pellets to yield Zn_3P_2 nanowires, sufficient amount of zinc should evaporate and then condense to form zinc droplets in zinc pellets. Since the quantity of zinc is very low in the zinc pellet, zinc foil can act as zinc source.

At the end of the experiment, zinc foil changed to yellow in color. Yellow color on the surface of the foil indicates the formation of Zn_3P_2 nanowires, similar to the results of previous work conducted by Brockway et.al [108]. In sharp contrast, zinc pellets have hardly changed their color. This implies that conditions suitable for the growth of nanowires on the zinc foil are not necessarily satisfactory to grow nanowires on the surfaces of the pellets even though the quantity of zinc in the pellet is very small compared to that in the foil.

4.3.2 Comparison of nanowire growth rate on the pellet to that on the foil

Comparison of growth rate between nanowires formed on foil and pellets is done as follows:

i. Two-run experiments using the conditions in table 2.

ii. Experimentation using the conditions in table 3.

Upon repetition of the experiment mentioned in section 4.3.1, few nanowires were formed on the pellets and zinc foil was dark yellow in color as indicated in figure 9 (a) and 9 (b). By varying the parameters such as hydrogen flow rate, phosphorus amount, and

substrate temperature, as indicated in table 3, it was possible to grow appreciable number of nanowires on the surface of the pellets as shown in the figure 10 (b). However, foil had changed to black color with diameters of wires in the range of few micrometers. These results indicate that, in comparison to the nanowire growth rate on the pellets, nanowires grow faster on the foil. Slower growth rate on the pellets could be due to the phosphorus diffusion limitation into the pellet or zinc diffusion limitation out of the pellet. It was also observed from these experiments that it is not possible to grow Zn_3P_2 nanowires both on the foil and pellets under the same experimental condition.

Table 3: Experimental conditions to compare the nanowire growth on the pellets to that on the foil by varying parameters such as hydrogen flow rate, substrate temperature, and phosphorus amount

Parameters	**Zone 1**	**Zone 2**	**Zone 3**
Temperature [°C]	410	410	485
Preheating time [minutes]	5	5	10
Reaction time [minutes]	40	40	35
Phosphorous quantity [mg]			1100

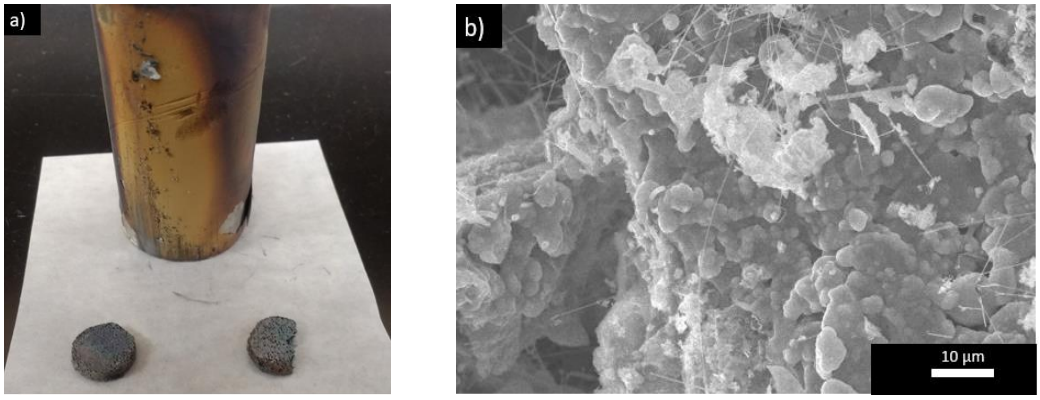

Figure 9: a) Photograph of zinc foil and pellets at the end of the two-run experiments using the conditions mentioned in table 2, b) SEM image of the pellet shows very few nanowires under this experimental condition

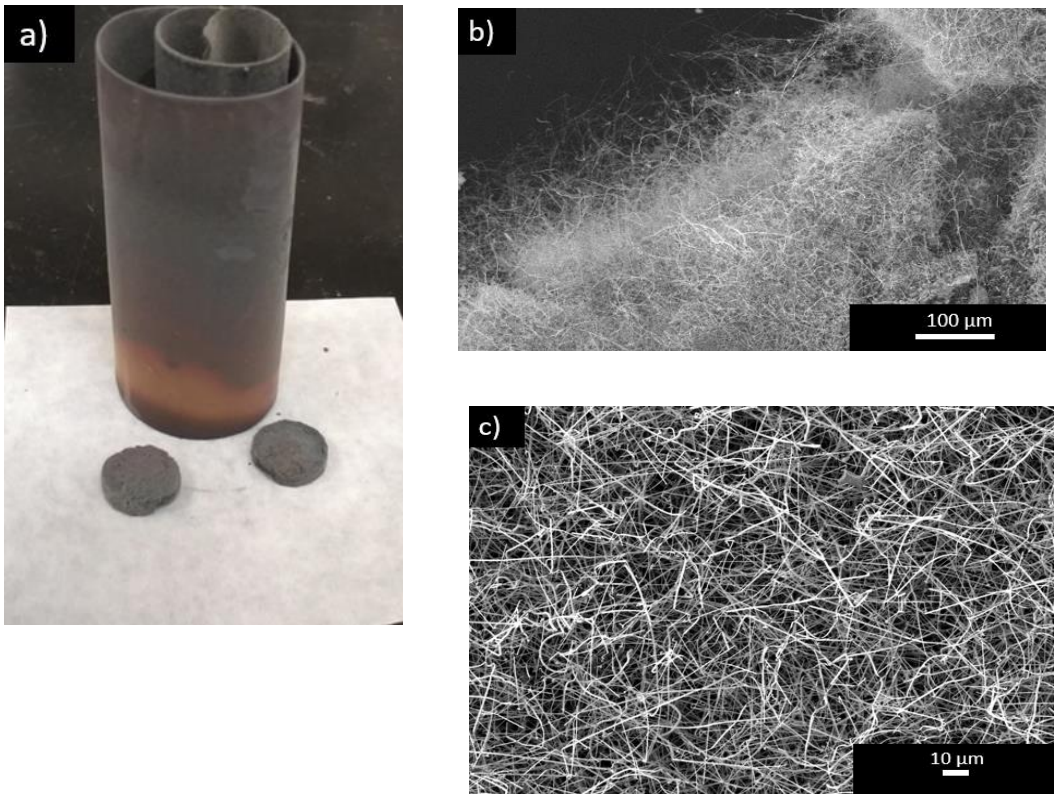

Figure 10: a) Photograph of resulting dark pellets and foil at experimental conditions mentioned in table 3, b) SEM image of the dark pellet shows very good number of nanowires on the surface, c) SEM image of the dark foil indicates wires with diameters in the range of few micrometers

4.3.3 Parameters affecting nanowire growth

Temperature

One of the requirements for the formation of compound material nanowires via VLS mechanism using low melting metal clusters such as zinc material is that the metal must be molten at the synthesis temperature [22]. The melting point of zinc is 419.5°C. Therefore, experiments were carried out at the substrate temperature in the range 400-420°C. It can be seen from the figure 11 that thicker nanowires were synthesized at a higher yield on the surface of the pellet at 420°C. This might be due to a higher vapor pressure of zinc to form many large droplets. Also, with the increase in temperature the dissolution rate of phosphorus in zinc droplet will increase. This could lead to higher supersaturation level of zinc phosphide to form thicker nanowires. However, at 420°C number of nanowires formed inside the pellet is less. This could be explained by the fact that, at 420°C zinc pellet collapses and loses its porous structure. This compromises the purpose of using NH_4Cl. Hence, 410°C is chosen as substrate temperature for this thesis.

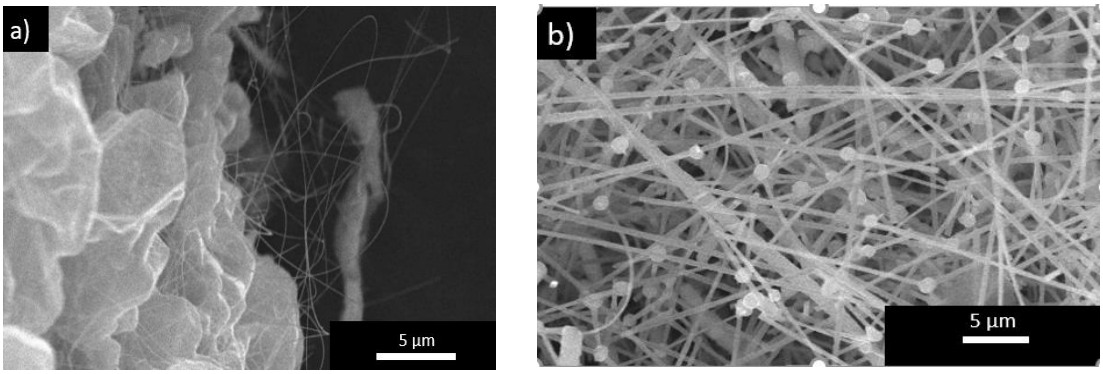

Figure 11: SEM images of resulting Zn_3P_2 pellets placed at zone 1 temperatures a) 400 °C and b) 420 °C. The analysis indicated that as the temperature increases, thicker nanowires at a higher yield is formed on the pellets

Zn: NH_4Cl ratio

The ratio of Zinc to NH_4Cl is an important factor in this study, given that the porosity of a pellet is dependent on the amount of NH_4Cl subliming. With a high ratio of Zinc to NH_4Cl, the pellet does not have enough pores for phosphorus vapors to diffuse through, which results in partially reacted inner region of pellets. SEM image in figure 12 (b) and 12 (c) indicate the decrease in number of nanowires in the inner region of the pellets with the increase in zinc to NH_4Cl ratio.

On the other hand, as shown in the figure 12 (a), with the decrease in weight ratio of Zinc to NH_4Cl, pellet loses its structural integrity to hold on to their porous structure after the sublimation of NH_4Cl from the pellet. This leads to lesser number of nanowires in the inner regions of the pellet. Since, phosphorus diffusion inside the pellet and zinc diffusion out of the pellet is stopped due to the unavailability of any pores. Accordingly, there is a trade-off in the ratio of Zinc to NH_4Cl. After series of experiments with different Zinc to

NH_4Cl weight ratio pellets, the ideal ratio for the nanowire growth was found to be 1:4 weight ratio of Zinc to NH_4Cl.

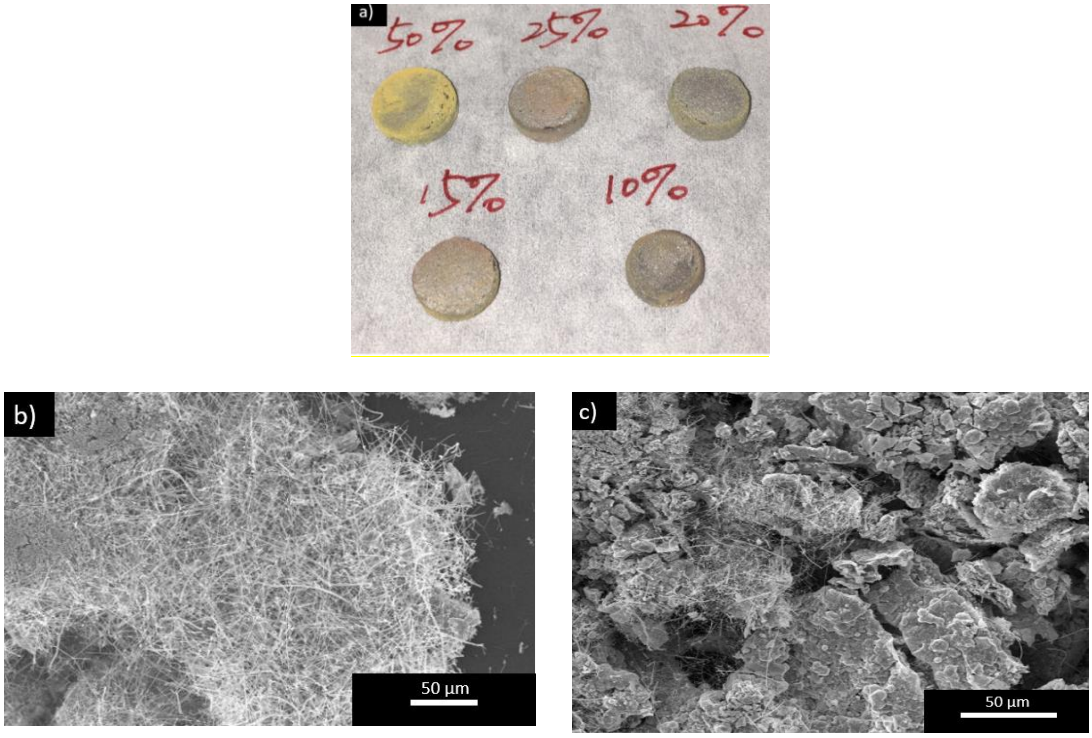

Figure 12: a) Optical micrographs of various weight ratio of zinc to NH_4Cl pellets at the end of experimental run. Percentage numbers in the figure indicates the ratio of weights of zinc to NH_4Cl in the beginning of the experiment. Figure indicates the decrease in structural integrity of the pellets with the decrease in zinc to NH_4Cl weight ratio. Scanning electron micrographs of b) Inner region of 25% by weight zinc/NH_4Cl pellet and c) Inner region 50% by weight zinc/NH_4Cl pellet. SEM images indicate that with the decrease in weight percentages of zinc/NH_4Cl, number of nanowires increases in the inner region of the pellet.

Preheating time

The evaporation rate of phosphorus in zone 3 of the reactor (figure 8 (b)) is increased by decreasing the preheating time, with the total reaction time to be constant. As the evaporation rate of phosphorus increases fewer nanowires are formed on zinc pellets.

This decrease in nanowire formation can be explained as follows. First, due to the lower latent heat carried by zinc pellets. The amount of zinc droplets formed increases with the increase in the vapor pressure of zinc. During the nanowire formation, phosphorus vapors dissolve in the zinc droplets which then react with zinc to form Zn_3P_2 [108]. Supersaturation of Zn_3P_2 leads to 1-D Zn_3P_2 nanowire growth from zinc droplets. If phosphorus powders are heated up quickly, then phosphorus reaches the substrate region earlier. In the initial heating stage of the pellet, NH_4Cl uses heat of evaporation to sublimate from the pellets. As a result heat for zinc to evaporate from the pellet is insufficient. This leads to a low vapor pressure of zinc and as a result few zinc phosphide nanowires are formed.

Second, with a high evaporation rate of red phosphorus it could react with NH_4Cl to form poly(dichlorophosphazane) [150], as shown below.

$$PCl_5 + NH_4Cl \rightarrow \frac{1}{n}(NPCl_2)_n + 4HCl$$

This parallel unpreffered reaction would lead to insufficent phosphorus vapors to react with the zinc droplets. Increase in carrier gas flowrate can also help in removing NH_4Cl out of the reactor to prevent this parallel reaction.

4.3.4 Experimentation without zinc foil

Zinc foil was used in the experiments to replicate the work conducted by Brockway *et al.* [108] , and to study different parameters affecting nanowire growth on the pellet. It was observed from the experiments that, for a given experimental condition it is impossible to grow nanowires on both the surface of the pellet and the foil at the same time. Hence, further studies were carried out without zinc foil. microscope glass slide was used to support pellets in the substrate section. In this experiment, the total weight of zinc was maintained similar to that of previous experiments by placing four pellets on microscope glass slides in the downstream of the reactor. Each zinc pellets (600 mg each) were prepared by mixing zinc flakes and ammonium chloride in 1:4 weight ratio. At the end of experiment, as shown in the figure 13, only the surface of the pellet is covered with Zn_3P_2 nanowires. To increase the nanowire yield inside the pellet, phosphorus should react with zinc completely. To ensure that, pellet thickness must be reduced which will decrease the phosphorus diffusion length. It was also observed from this experiment that the final weight of the pellets was less when pellets were placed on glass slides when compared to that on zinc foil. This is due to the less zinc source in the vapor phase to form zinc droplets. In the following chapter, experiments with thin zinc pellets have been discussed to completely convert zinc pellet to zinc phosphide nanowires without any byproducts.

Table 4: Experimental conditions for a trial with four zinc pellets on a microscope glass slide

Parameters	**Zone 1**	**Zone 2**	**Zone 3**
Temperature [°C]	410	410	485
Preheating time [minutes]	10	10	25
Reaction time [minutes]	35	35	20
Phosphorous quantity [mg]			300
Hydrogen flow rate [sccm]	100		

Figure 13: Photograph of the pellet with nanowires only on the surface of the pellet. The inner region of the pellet was found to have some unreacted zinc material along with Zn_3P_2 nanowires

CHAPTER V

OPTIMAL EXPERIMENTAL CONDITIONS FOR ZINC PHOSPHIDE NANOWIRE SYNTHESIS ON ZINC PELLETS

5.1 Introduction

In this chapter, the method to efficiently synthesize Zn_3P_2 nanowires in large quantities has been described. To accomplish this objective thin zinc/NH_4Cl mixture pellets with a larger diameter were used as the substrate material. Scanning electron microscopy (SEM) and X-Ray Diffraction (XRD) analysis techniques were used to determine the morphology and compositions of the final product respectively.

5.2 Methods

Zinc flakes and NH_4Cl powders were mixed and ground using mortar and pestle at a weight ratio of 1:4. The powder mixture was then consolidated into pellets by uniaxial pressing at a pressure of 76 MPa. Resulting zinc/ NH_4Cl mixture pellets were 2 cm in diameter, 1-2 mm thickness, and weighed 800 mg. Three such large, thin zinc/ NH_4Cl mixture pellets were placed on a microscope glass slide at the downstream of the CVD reactor as shown in figure 14 (a). 300 mg of red phosphorus was placed in a porcelain crucible at upstream of the reactor. The reactor was operated at a pressure ranging 200-700 mTorr. Hydrogen gas (carrier gas) was introduced at a flow rate of 100 sccm. Each zone in the reactor was heated to the desired temperature as listed in table 5. At the end of the experiment, the reactor was cooled rapidly. Final nanowire product was characterized using SEM (JEOL JSM-7500F) and XRD (Bruker-AXS D8).

Table 5: Optimal conditions for the synthesis of Zn_3P_2 nanowires on zinc pellets.

Parameters	**Zone 1**	**Zone 2**	**Zone 3**
Temperature [°C]	410	410	485
Preheating time [minutes]	5	5	25
Reaction time [minutes]	40	40	20

5.3 Results and discussion

Figures 14 (b) and 14 (c) depict the change in color of pellets from grey before the reaction to yellow after the reaction. The yellow color indicates Zn_3P_2 nanowires on the pellet. 2.4 g of mixture of zinc and NH_4Cl pellets yielded 100 mg of Zn_3P_2 nanowires. Percentage yield of Zn_3P_2 nanowires per gram zinc metal basis is calculated to be approximately 20.8%. Figures 15 (a) and 15 (b) show the SEM image of the surface regions and figures 15 (c) and 15 (d) show the SEM image of the inner regions of pellets. It can be observed that entire pellet has converted into Zn_3P_2 nanowires with diameters ranging from 90-120 nm and lengths up to 100 μm.

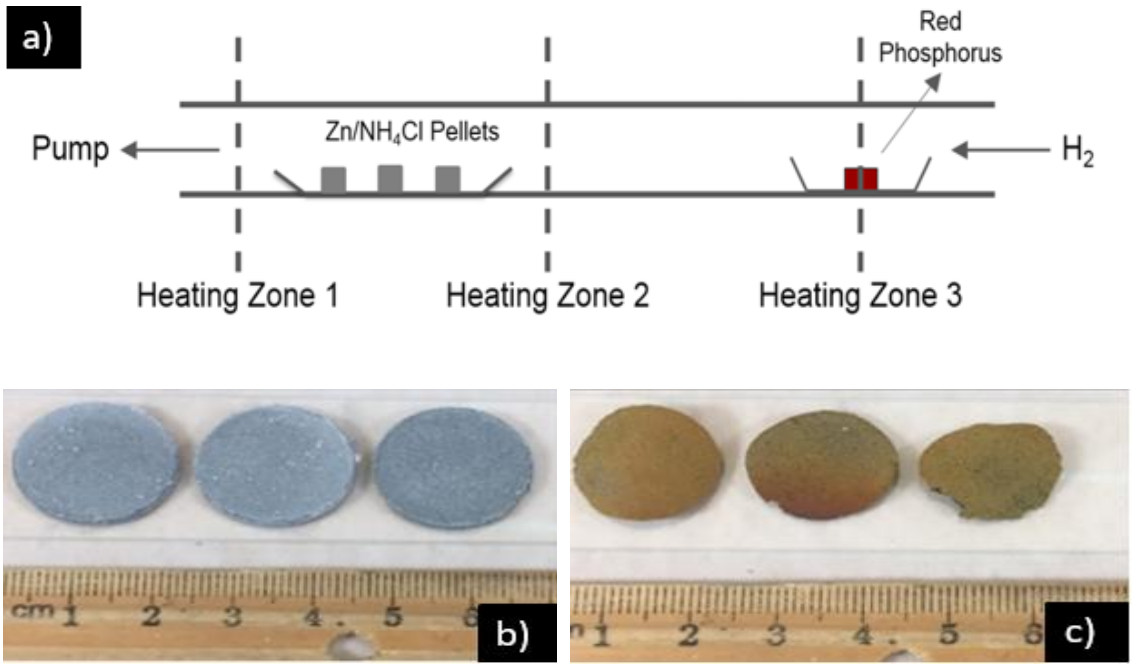

Figure 14: (a) Schematic illustration of CVD setup for the synthesis of Zn_3P_2 nanowires on zinc pellets. Camera photos, (b) zinc pellets before the experiment and (c) Zn_3P_2 nanowire pellets synthesized by the reaction of zinc pellets with red phosphorous

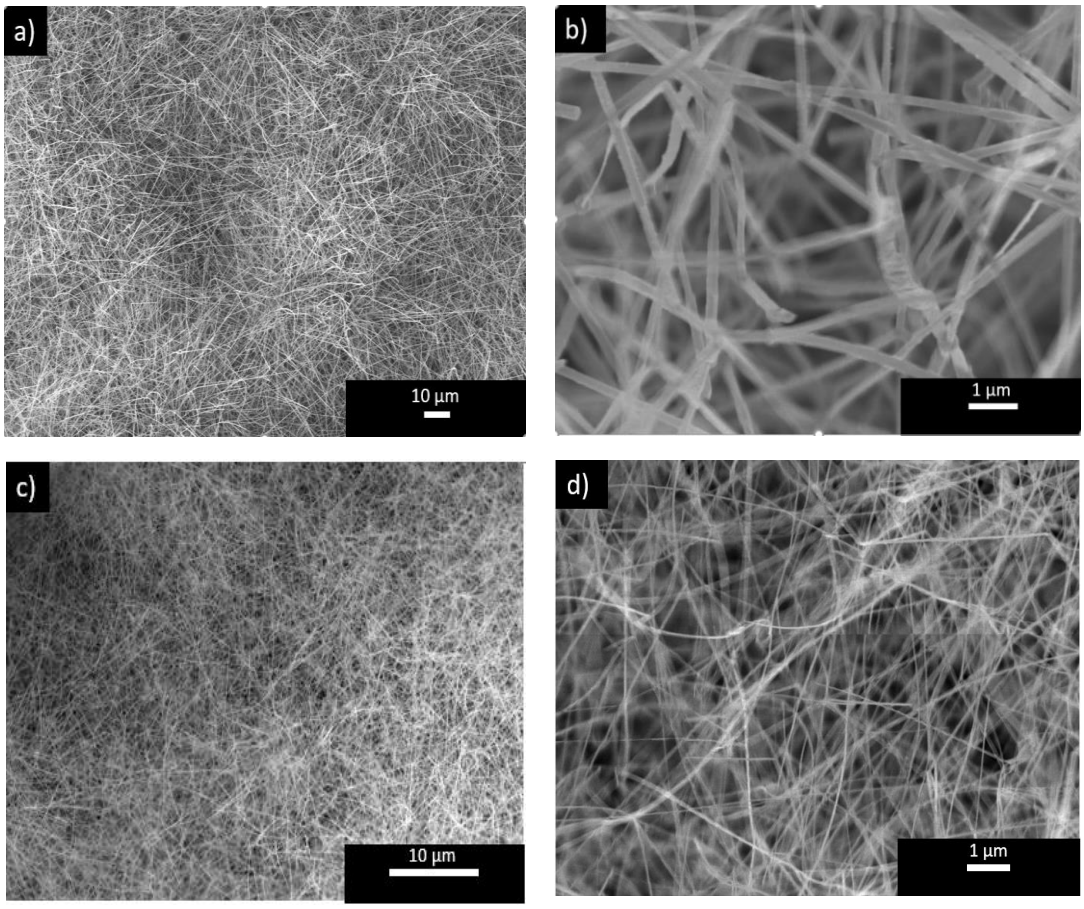

Figure 15: Scanning electron microscopes of (a) The surface image of Zn_3P_2 nanowire pellet and (b) magnified surface image of Zn_3P_2 pellet (c) image of inner region of the Zn_3P_2 pellet and (d) magnified image of inner region of the pellet

Nanowire growth mechanism

Zinc phosphide nanowires are grown on zinc pellets by preheating and reaction steps. In the preheating step, micropores and nanopores are formed on the zinc pellets. Zinc droplets in zinc pellets react with phosphorus vapor to form Zn_3P_2 nanowires on pellets during the reaction step. Nanowire growth procedure is schematically represented in figure 16 (a).

Initially during preheating step, zinc pellets are heated to 410°C for 25 minutes. Due to the low sublimation point of NH_4Cl, it decomposes into NH_3 and HCl gases at 338°C leaving behind porous zinc pellets [151]. A control experiment was conducted on NH_4Cl pellets by heating them to 410°C for different duration under the atmospheric pressure. It was observed that entire NH_4Cl pellet was evaporated in 20 minutes. Hence, it can be assumed that NH_4Cl will be mostly evaporated from zinc pellets after heating for 25 minutes. An SEM image on preheated zinc pellet in figure 16 (c) and 16 (d) show the formation of pores on the pellets, with dimensions ranging from a few micrometers to a few hundred nanometers. Zinc pellets were able to maintain its structure even after preheating.

During reaction step, zinc phosphide nanowires are presumed to be formed by self-catalysis explained previously by Brockway *et al* [108]. Red phosphorus evaporates and the carrier gas transports phosphorus vapors towards the zinc pellets. At the substrate section, zinc vapors react with phosphorous vapors and condense to form Zn_3P_2 crystal nuclei. Selective wetting of the nuclei with zinc causes the formation of zinc droplets, and finally, liquid phase epitaxy (LPE) through the zinc droplets leads to the formation of Zn_3P_2 nanowires.

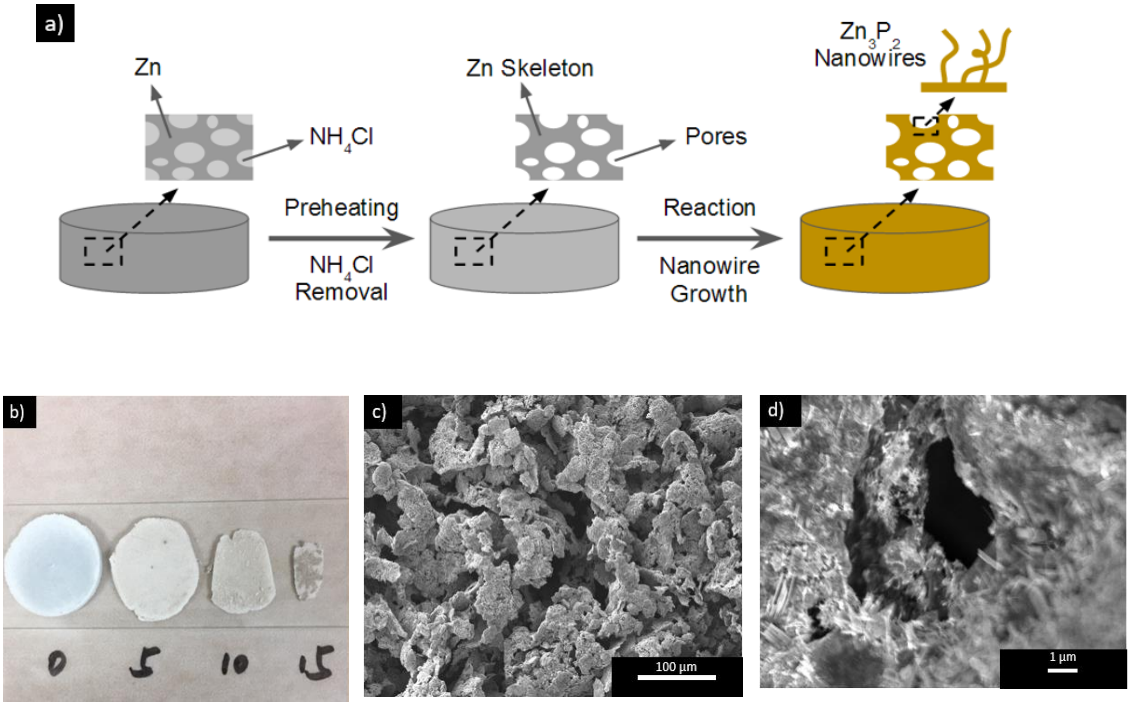

Figure 16: (a) Schematic illustration of different steps involved in Zn_3P_2 nanowire growth on the zinc pellet. (b) Camera image of NH_4Cl pellets after heating on a glass substrate at 410 °C for various time interval (Numbers in the figure represents time in minutes), (c) SEM image of surface of the pellet after heating for 25 minutes at 410 °C, (d) magnified SEM image of figure 16 (c), shows micropores and nanopores. The dimension of the nanopores are in the order of a few hundred nanometers.

Nanopores and robust structure of the preheated pellets help phosphorus vapor to diffuse into the inner regions of the pellet. Hence, the entire zinc pellet reacts with phosphorus vapors to form Zn_3P_2 nanowires. In figure 17, the XRD analysis of the final product confirmed that the pellets are purely composed of tetragonal Zn_3P_2 with lattice parameters of a = 8.095 Å and c = 11.47 Å. No other impurities or byproducts such as Zn,

ZnO, $ZnCl_2$, and NH_4Cl were detected. Hence, it can be confirmed that the entire pellets were converted to Zn_3P_2 nanowires.

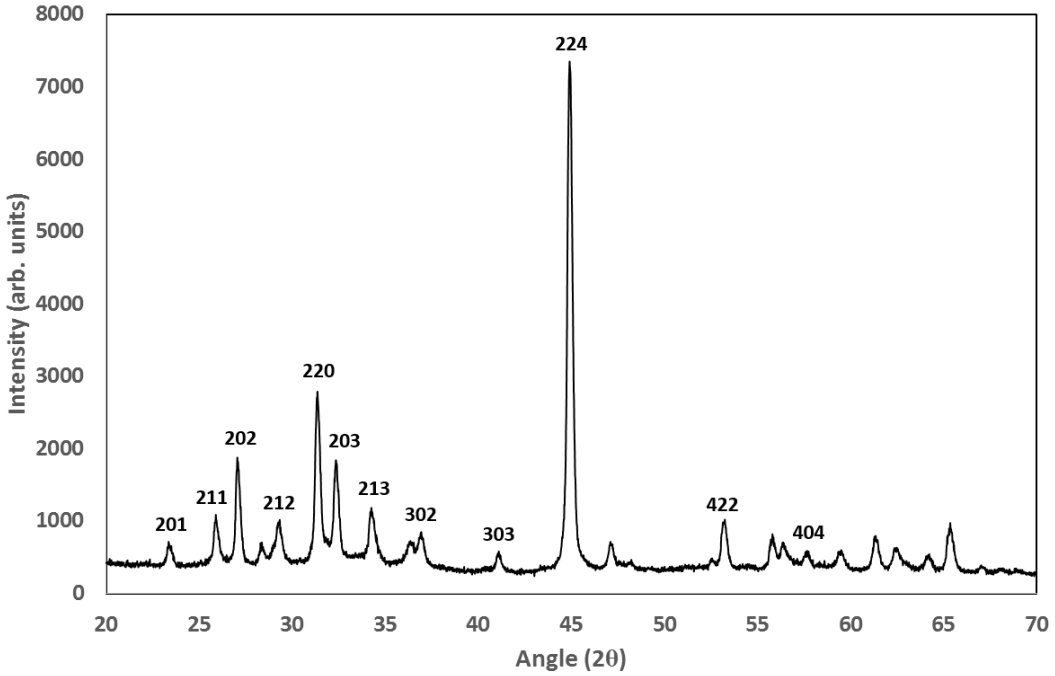

Figure 17: Post-synthesis XRD spectrum of the powdered sample of the pellets shown in figure 14 (c). The sample displays characteristic peaks of tetragonal Zn_3P_2

CHAPTER VI

CONCLUSIONS

The main objective of this thesis is to achieve large-scale synthesis of Zn_3P_2 nanowires in a contaminant-free and byproduct-free manner. Previously, Zn_3P_2 nanowires have been synthesized using zinc foils as substrate in CVD chamber. However, this method is not feasible for commercial nanowire synthesis due to wastage of zinc substrate as the nanowire formation is constrained only to the surface of the zinc substrate. In addition, the nanowire removal process is physically challenging and time-intensive.

The following is the summary of the results that form the core of this thesis:

- Zinc/NH_4Cl mixture pellets were used as the substrate materials as a strategy to increase thermal conductivity and phosphorus diffusion in order to convert the entire zinc pellet into Zn_3P_2 nanowires giving a yield of 20.8% compared to 1.56% demonstrated previously by Brockway *et al*.
- This process is scalable. Hence, Zn_3P_2 nanowires could be synthesized in large quantities in addition to reduction in post-synthesis (nanowire collection) time.
- Higher quality nanowires have been obtained. XRD analysis of the final product confirmed that the resulting Zn_3P_2 pellets are devoid of any contaminants such as Zn, ZnO, or NH_4Cl. In addition, SEM analysis confirms lack of unwanted Zn_3P_2 bulk material or other nanostructures in the final product.

- It was also demonstrated that factors such as Zn to NH_4Cl ratio and phosphorus pre-heating time have shown to have impact on the quantity and quality of Zn_3P_2 nanowires.

REFERENCES

[1] G. Guisbiers, S. Rosales and F. Deepak, "Nanomaterial Properties: Size and Shape Dependencies," *J. Nanomater,* vol. 2012, pp. 1-2, 2012.

[2] J. Kimling, M. Maier, B. Okenve, V. Kotaidis, H. Ballot and A. Plech, "Turkevich Method for Gold Nanoparticle Synthesis Revisited," *J. Phys. Chem. B,* vol. 110, pp. 15700-15707, 2006.

[3] Y. Wang and A. Hu, "Carbon quantum dots: synthesis, properties and applications," *J. Mater. Chem. C,* vol. 2, pp. 6921-6939, 2014.

[4] W. I. Park, D. H. Kim and S. Jung, "Metalorganic vapor-phase epitaxial growth of vertically well-aligned ZnO nanorods," *Appl. Phys. Lett.*, vol. 80, no. 22, pp. 4232-4234, 2002.

[5] A. Morales and C. Lieber, "A Laser Ablation Method for the Synthesis of Crystalline Semiconductor Nanowires," *Science,* vol. 279, no. 5348, pp. 208-211, 1998.

[6] C. Journet, W. Maser, P. Bernier, A. Loiseau and S. Lefrant, "Large-scale production of single-walled carbon nanotubes by the electric-arc technique," *Nature,* vol. 388, pp. 756-758, 1997.

[7] L. Mai, B. Hu, W. Chen, Y. Qi, C. Lao, R. Yang, Y. Dai and Z. Wang, "Lithiated MoO3 Nanobelts with Greatly Improved Performance for Lithium Batteries," *Adv. Mater.*, vol. 19, no. 21, pp. 3712-3716, 2007.

[8] X. Li, W. Cai, J. An and S. Kim, "Large-Area Synthesis of High-Quality and Uniform Graphene Films on Copper Foils," *Science,* vol. 324, no. 5932, pp. 1312-1314, 2009.

[9] G. Eda, G. Fanchini and M. Chhowalla, "Large-area ultrathin films of reduced graphene oxide as a transparent and flexible electronic material," *Nat Nanotechnol.,* vol. 3, pp. 270-274, 2008.

[10] E. Drexler and D. Pamlin, The Birth of Nanotechnology: From Visionary Idea to World-Wide Research Delivering Initial Results in 50 years, Nano, 2013.

[11] M. Reibold, P. Paufler, A. Levin, W. Kochmann, N. Patzke and a. D. Meyer, "Materials: carbon nanotubes in an ancient Damascus sabre," *Nature,* vol. 444, p. 286, 2006.

[12] NNI, "National Nanotechnology Initiative," Official website of the United States National Nanotechnology Initiative, 2017. [Online]. Available: http://www.nano.gov/.

[13] H. Kang, "A review of the emerging nanotechnology industry: materials, fabrications, and applications.," 2010. [Online]. Available: https://www.dtsc.ca.gov/TechnologyDevelopment/Nanotechnology/upload/Review_of_Emerging_Nanotech_Industry.pdf.

[14] A. Nikalje, "Nanotechnology and its Applications in Medicine," *Med chem,* vol. 5, pp. 81-89, 2015.

[15] A. Rae, "Real Life Applications of Nanotechnology in Electronics," 2005. [Online]. Available: http://www.onboard-technology.com/pdf_ottobre2005/100507.pdf.

[16] T. Dhewa, "Nanotechnology Applications In Agriculture: An Update," *Oct. Jour. Env. Res. Vol.* , vol. 3, no. 2, pp. 204-211, 2015.

[17] W. Luther, Applications of Nanotechnologies in the Energy Sector, Dusseldorf: HA Hessen Agentur, 2008.

[18] M. Pitkethly, "Nanomaterials- the driving force," *Materials Today,* vol. 7, no. 12, pp. 20-29, 2004.

[19] NNI, "National Nanotechnology Initiative Strategic Plan," 2016. [Online]. Available: https://www.nano.gov/sites/default/files/pub_resource/2016-nni-strategic-plan.pdf.

[20] X. Zhao, C. Wei, L. Yang and M. Chou, "Quantum Confinement and Electronic Properties of Silicon Nanowires," *Phys. Rev. Lett.*, vol. 92, no. 23, pp. 236805 1-4, 2004.

[21] C. Lieber, "The Incredible Shrinking Circuit," *Sci Am,* pp. 59-64, 2001.

[22] M. Meyyappan and M. Sunkara, Inorganic Nanowires, Taylor & Francis Group, 2009.

[23] ABNEWSWIRE, "Silver nanowire market estimated to reach USD 408.14 million by 2021," 17 May 2017. [Online]. Available: http://www.abnewswire.com/pressreleases/silver-nanowire-market-estimated-to-reach-usd-40814-million-by-2021_116827.html.

[24] SIGMA-ALDRICH. [Online]. Available: http://www.sigmaaldrich.com/united-states.html.

[25] Y. Cui, X. Duan, Y. Huang and C. Lieber, "Nanowires as Building Blocks for Nanoscale Science and Technology," in *Nanowires and Nanobelts: Materials, Properties, and Devices*, Boston, Kluwer Academic Publishers, 2003, pp. 3-65.

[26] U. Cvelbar, "Towards large-scale plasma-assisted synthesis of nanowires," *J. Phys. D: Appl. Phys.*, vol. 44, p. 174014, 2011.

[27] C. Chan, H. Peng, G. Liu and Y. Cui, "High-performance lithium battery anodes using silicon nanowires," *Nat Nanotechnol*, vol. 3, pp. 31-35, 2008.

[28] K. Peng, J. Jie, W. Zhang and S. Lee, "Silicon nanowires for rechargeable lithium-ion battery anodes," *Appl. Phys. Lett.*, vol. 93, pp. 033105 1-3, 2008.

[29] J. Dunn, L. Gaines, M. Barnes and M. Wang, "Material and Energy Flows in the Materials Production, Assembly, and End-of-Life Stages of the Automotive Lithium-Ion Battery Life Cycle," Argonne national laboratory, pennsylvania, 2012.

[30] L. Cui, Y. Yang and Y. Cui, ""Carbon-Silicon Core-Shell Nanowires as High Capacity Electrode for Lithium Ion Batteries," *Nano Lett.*, vol. 9, no. 9, pp. 3370-3374, 2009.

[31] IEA, "Global EV Outlook 2016: Beyond one million electric cars," 2016. [Online]. Available: https://www.iea.org/publications/freepublications/publication/Global_EV_Outlook_2016.pdf.

[32] Lipomi, J. Darren, R. Martinez and M. Kats, "Patterning the Tips of Optical Fibers with Metallic Nanostructures Using Nanoskiving," *Nano Lett.*, vol. 11, no. 2, pp. 632-636, 2011.

[33] B. Xia, H. Wu and Y. Yan, "Ultrathin and Ultralong Single-Crystal Platinum Nanowire Assemblies with Highly Stable Electrocatalytic Activity," *J. Am. Chem. Soc.*, vol. 135, no. 25, pp. 9480-9485, 2013.

[34] W. Bu, Z. Hua, L. Zhang and H. Chen, "Surfactant-assisted synthesis of lanthanide phosphates," *J. Mater. Res*, vol. 10, no. 10, pp. 2807-2811, 2004.

[35] D. Huong, L. Trang, L. Vu and N. Long, "Structural and optical properties of terbium doped lanthanum orthophosphate nanowires synthesized by hydrothermal method," *J. Alloys Compd.*, vol. 602, p. 306–311, 2014.

[36] A. Cao and E. J. R. Sudholter, "Silicon Nanowire-Based Devices for Gas-Phase Sensing," *Sensors*, vol. 14, pp. 245-271, 2014.

[37] Y. Li, F. Qian, J. Xiang and C. Lieber, "Nanowire electronic and optoelectronic devices," *Mater. Today,* vol. 9, pp. 18-27, 2006.

[38] B. Li, C. Chen, U. Kumar and Y. Chen, " Advances in nanowire transistors for biological analysis and cellular investigation," *Analyst* , vol. 139, pp. 1589-1608, 2014.

[39] S. Logothetidis, "Flexible organic electronic devices: Materials, process and applications," *Materials Science and Engineering B,* vol. 152, pp. 96-104, 2008.

[40] Y. Sun and J. Rogers, "Inorganic Semiconductors for Flexible Electronics," *Adv. Mater.,* vol. 19, pp. 1897-1916, 2007.

[41] J. Lee, A. Wang and Y. Rheem, "DNA Assisted Assembly of Multisegmented Nanowires," *Electroanalysis,* vol. 19, no. 22, pp. 2287 - 2293 , 2007.

[42] N. Kovtyukhova and T. Mallouk, "Nanowires as Building Blocks for Self-Assembling Logic and Memory Circuits," *Chem. Eur. J.,* vol. 8, no. 19, pp. 4354-4363, 2002.

[43] Y. Huang, X. Duan and C. Lieber, "Directed assembly of one-dimensional nanostructures into functional networks," *Science,* vol. 291, no. 5504, pp. 630-3, 2001.

[44] G. Yu, X. Li and C. Lieber, "Nanomaterial-incorporated blown bubble films for large-area, aligned nanostructures," *J. Mater. Chem.,* vol. 18, pp. 728-734, 2008.

[45] K. Heo, E. Cho, J. Yang, M. Kim and M. Lee, "Large-Scale Assembly of Silicon Nanowire Network-Based Devices Using Conventional Microfabrication Facilities," *Nano Lett.,* vol. 8, no. 12, p. 4523–4527, 2008.

[46] S. Myung, M. Lee, G. Kim and J. Ha, "Large-Scale “Surface-Programmed Assembly” of Pristine Vanadium Oxide Nanowire-Based Devices," *Adv. Mater.,* vol. 17, no. 19, pp. 2361-2364, 2005.

[47] S. Lee, M. Jeong and J. Myoung, "Magnetic alignment of ZnO nanowires for optoelectronic device applications," *Appl. Phys. Lett,* vol. 90, pp. 133115 1- 3 , 2007.

[48] B. Yoo, Y. Rheem and W. Beyermann, "Magnetically assembled 30 nm diameter nickel nanowire with ferromagnetic electrodes," *Nanotechnology,* vol. 17, no. 10, pp. 2512-2517, 2006.

[49] M. Wang and B. Gates, "Directed assembly of nanowires," *materials today*, vol. 12, no. 5, pp. 34-43, 2009.

[50] C. Mayousse, C. Celle and A. Fraczkiewics, "Stability of silver nanowire based electrodes under environmental and electrical stresses," *Nanoscale*, vol. 7, pp. 2107-2115, 2015.

[51] W. Zhou, X. Dai and T. Fu, "Long Term Stability of Nanowire Nanoelectronics in Physiological Environments," *Nano Lett.*, vol. 14, no. 3, pp. 1614-1619, 2014.

[52] C. Chan, H. Peng, G. Liu and X. Feng, "High-performance lithium battery anodes using silicon nanowires," *Nature Nanotechnology*, vol. 3, pp. 31-35, 2008.

[53] Y. Cui, L. Lauhon, M. Gudiksen and C. L. J Wang, "Diameter-controlled synthesis of single-crystal silicon nanowires," *Appl. Phys. Lett.*, vol. 78, no. 15, pp. 2214-2216, 2001.

[54] J. Rimstidt and H. Barnes, "The kinetics of silica-water reactions," *Geochim. Cosmochim. Acta*, vol. 44, no. 11, pp. 1683-1699, 1980.

[55] F. Patolsky, B. Timko, G. Yu and Y. Fang, "Detection, Stimulation, and Inhibition of Neuronal Signals with High-Density Nanowire Transistor Arrays," *Science*, vol. 313, no. 5790, pp. 1100-1104, 2006.

[56] N. Nesakumar, K. Thandavan and S. Sethuraman, "An electrochemical biosensor with nanointerface for lactate detection based on lactate dehydrogenase immobilized on zinc oxide nanorods," *J. Colloid Interface Sci.*, vol. 414, pp. 90-96, 2014.

[57] M. Willander, O. Nur, Q. Zhao and L. Y. B. Cao, "Zinc oxide nanorod based photonic devices: recent progress in growth, light emitting diodes and lasers," *Nanotechnology*, vol. 20, p. 332001, 2009.

[58] K. Adlkofer, W. Eck and M. Grunze, "Surface engineering of gallium arsenide with 4-mercaptobiphenyl monolayers," *J. Phys. Chem. B*, vol. 107, pp. 587-591, 2003.

[59] N. Myung, Y. Bae and A. Bard, "Effect of surface passivation on the electrogenerated chemiluminescence of CdSe/ZnSe nanocrystals," *Nano Lett.*, vol. 3, pp. 1053-1055, 2003.

[60] V. Holmberg, M. Rasch and B. Korgel, "PEGylation of Carboxylic Acid-Functionalized Germanium Nanowires," *Langmuir*, vol. 26, pp. 14241-14246, 2010.

[61] V. Vasiraju, Y. Kang and S. Vaddiraju, "Non-conformal decoration of semiconductor nanowire surfaces with boron nitride (BN) molecules for stability enhancement: degradation-resistant Zn3P2, ZnO and Mg2Si nanowires," *Phys. Chem. Chem. Phys*, vol. 16, pp. 16150-16157, 2014.

[62] M. D. Groner, F. H. Fabreguette, J. Elam and S. M. George, "Low-Temperature Al2O3 Atomic Layer Deposition," *Chem. Mater.*, vol. 16, no. 4, pp. 639-645, 2004.

[63] C. MA, Y. Berta and Z. Wang, "Patterned aluminum nanowires produced by electron beam at the surfaces of AlF3 single crystals," *Solid State Commun.*, vol. 129, pp. 681-685, 2004.

[64] H. Wu, L. Stern, J. Chen and P. Rack, "Synthesis of nanowires via helium and neon focused ion beam induced deposition with the gas field ion microscope," *Nanotechnology,* vol. 24, no. 17, 2013.

[65] D. Wouters and U. Schubert, "Nanolithography and nanochemistry: probe-related patterning techniques and chemical modification for nanometer-sized devices," *Angew Chem Int Ed Engl,* vol. 43, no. 19, pp. 2480-2495, 2004.

[66] Z. Wang, J. Liu, X. Chen, J. Wan and Y. Qian, "A simple hydrothermal route to large-scale synthesis of uniform silver nanowires.," *Chem. Eur. J.*, vol. 11, no. 1, pp. 160-3, 2004.

[67] D. Holmes, P. Johnston, R. Doty and B. Korgel, "Control of thickness and orientation of solution-grown silicon nanowires," *Science,* vol. 287, no. 5457, pp. 1471-1473, 2000.

[68] U. Gomes, D. Ercolani, V. Zannier, F. Beltram and L. Sorba, "Nucleation and growth mechanism of self-catalyzed InAs nanowires on silicon," *Nanotechnology,* vol. 27, no. 25, pp. 255601(1-7), 2016.

[69] B. Mandl, J. Stangl, E. Hilner, A. Zakharov and A. Mikkelsen, "Growth Mechanism of Self-Catalyzed Group III−V Nanowires," *Nano Lett.*, vol. 10, no. 11, pp. 4443-4449, 2010.

[70] B. Gates, Q. Xu, M. Stewart, D. Ryan and G. Whitesides, "New Approaches to Nanofabrication: Molding, Printing, and Other Techniques," *Chem. Rev.*, vol. 105, no. 4, pp. 1171-1196, 2005.

[71] P. Namdari, H. Daraee and A. Eatemadi, "Recent Advances in Silicon Nanowire Biosensors: Synthesis Methods, Properties, and Applications," *Nanoscale Res Lett.,* vol. 11, no. 406, pp. 1-16, 2016.

[72] Y. Xia, P. Yang, Y. Sun, Y. Wu, B. Mayers, B. Gates, Y. Yin, F. Kim and H. Yan, "One-Dimensional Nanostructures: Synthesis, Characterisation, and Applications," *Adv. Mater,* vol. 15, no. 5, pp. 353-389, 2003.

[73] T. Trentler, K. Hickman, S. Goel, A. Viano, P. Gibbons and W. Buhro, "Solution-Liquid-Solid Growth of Crystalline III-V Semiconductors: An Analogy to Vapor-Liquid-Solid Growth," *Science,* vol. 270, pp. 1791-1794, 1995.

[74] B. Kaushik, S. Verma, A. Kulkarni and S. Prajapati, Next Generation Spin Torque Memories, Singapore: Springer Nature, 2017.

[75] H. Espinosa and G. Bao, Nano and Cell Mechanics: Fundamentals and Frontiers, United Kingdom: John Wiley & Sons Ltd, 2013.

[76] M. Stan, P. Franzon, S. Goldstein and M. Ziegler, "Molecular Electronics: From Devices and Interconnect to Circuits and Architecture," *Proceedings of the IEEE,* vol. 91, no. 11, pp. 1940-1957, 2003.

[77] S. De, T. Higgins and P. Lyons, "Silver Nanowire Networks as Flexible, Transparent, Conducting Films: Extremely High DC to Optical Conductivity Ratios," *ACS Nano,* vol. 3, no. 7, pp. 1767-1774, 2009.

[78] T. Kim, Y. Kim, H. Lee, H. Kim and W. Yang, "Uniformly interconnected silver-nanowire networks for transparent film heaters," *Adv. Funct. Mater.,* vol. 23, no. 10, pp. 1250-1255, 2013.

[79] J. Emmott, A. Urbina and J. Nelson, "Environmental and economic assessment of ITO-free electrodes for organic solar cells," *Sol. Energy Mater. Sol. Cells,* vol. 97, pp. 14-21, 2012.

[80] J. Ye and L. Qi, "Solution-phase Synthesis of One-dimensional Semiconductor Nanostructures," *J. Mater. Sci. Technol,* vol. 24, no. 4, pp. 529-540, 2008.

[81] Z. Li, X. Huang, J. Liu and H. Ai, "Single-crystalline ZnO nanowires on zinc substrate by a simple hydrothermal synthesis method," *Mater. Lett.,* vol. 62, no. 16, pp. 2507-2511, 2008.

[82] D. Kumar, S. Srivastava, P. Singh, K. Sood, V. Singh, N. Dilawar and M. Husain, "Room temperature growth of wafer-scale silicon nanowire arrays and their Raman characteristics," *J Nanopart Res,* vol. 12, pp. 2267-2276, 2010.

[83] K. Byrappa and M. Yoshimura, Handbook of Hydrothermal Technology: second edition, Oxford: Elsevier, 2013.

[84] C. Xu, Y. Wang, H. Chen, R. Zhou and Y. Liu, "Large-scale synthesis of ultralong copper nanowires via a facile ethylenediamine-mediated process," *J. Mater. Sci. - Mater. Electron.*, vol. 25, no. 5, p. 2344–2347, 2014.

[85] B. Gates, B. Mayers, B. Cattle and Y. Xia, "Synthesis and characterization of uniform nanowires of trigonal selenium," *Adv. Funct. Mater.*, vol. 12, no. 3, p. 219, 2002.

[86] B. Bhushan, Springer Handbook of Nanotechnology, Springer, 2006.

[87] S. Li, Y. Chen, L. Huang and D. Pan, "Large-Scale Synthesis of Well-Dispersed Copper Nanowires in an Electric Pressure Cooker and Their Application in Transparent and Conductive Networks," *Inorg. Chem.*, vol. 53, pp. 4440-4444, 2014.

[88] J. Chen, T. Herricks, M. Giessler and Y. Xia, "Single-Crystal Nanowires of Platinum Can Be Synthesized by Controlling the Reaction Rate of a Polyol Process," *J. Am. Chem. Soc.*, vol. 126, no. 35, pp. 10854-10855, 2004.

[89] M. Tsuji, M. Hashimoto, Y. Nishizawa and T. Tsuji, "Synthesis of gold nanorods and nanowires by a microwave–polyol method," *Mater. Lett.*, vol. 58, pp. 2326-2330, 2004.

[90] X. Liang, T. Zhao, Y. Hu, P. Zhu, R. Sun, D. Lu and C. Wong, "CuCl2 and stainless steel synergistically assisted synthesis of high-purity silver nanowires on a large scale," *RSC Adv.*, vol. 4, pp. 47536-47539, 2014.

[91] H. Ding, Y. Zhang, G. Yang, S. Zhang and P. Zhang, "Large scale preparation of silver nanowires with different diameters by a one-pot method and their application in transparent conducting films," *RSC Adv*, vol. 6, pp. 8096-8102, 2016.

[92] Y. Sun, B. Mayers, T. Herricks and Y. Xia, "Polyol Synthesis of Uniform Silver Nanowires: A Plausible Growth Mechanism and the Supporting Evidence," *Nano Lett.*, vol. 3, no. 7, pp. 955-960, 2003.

[93] T. Trentler, K. Hickman, S. Goel, A. Viano, P. Gibbons and W. Buhro, "Solution-liquid-solid growth of crystalline III-V semiconductors: An analogy to vapor-liquid-solid growth," *Science*, vol. 270, pp. 1791-1794, 1995.

[94] F. Wang, A. Dong and W. Buhro, "Solution−Liquid−Solid Synthesis, Properties, and Applications of One-Dimensional Colloidal Semiconductor Nanorods and Nanowires," *Chem. Rev.*, vol. 116, pp. 10888-10933, 2016.

[95] F. Wang, A. Dong, J. Sun, H. Yu and W. Buhro, "Solution-Liquid-Solid Growth of Semiconductor Nanowires," *Inorg. Chem.*, vol. 45, pp. 7511-7521, 2006.

[96] A. Dong, H. Yu, F. Wang and W. Buhro, "Colloidal GaAs Quantum Wires: Solution-Liquid-Solid Synthesis and Quantum-Confinement Studies," *J. Am. Chem. Soc*, vol. 130, pp. 5954-5961, 2008.

[97] M. Zhang, K. Peng, X. Fan, J. Jie, R. Zhang and N. Wong, "Preparation of Large-Area Uniform Silicon Nanowires Arrays through Metal-Assisted Chemcial Etching," *J. Phys. Chem. C*, vol. 112, pp. 4444-4450, 2008.

[98] A. Hochbaum, D. Gargas, Y. Hwang and a. P. Yang, "Single Crystalline Mesoporous Silicon Nanowires," *Nano Lett.*, vol. 9, no. 10, pp. 3550-3554, 2009.

[99] F. Xu, L. Zhang and Y. Zhu, "A Growth Mechanism for 1D Nanocrystals: Pseudoscrew Packing of Polyhedral Growth Units," *Cryst. Growth Des.*, vol. 8, no. 7, pp. 2574-2580, 2008.

[100] M. Law, J. Goldberger and P. Yang, "Semiconductor Nanowires and Nanotubes," *Annu. Rev. Mater. Res.*, vol. 34, pp. 83-122, 2004.

[101] J. Chen, Q. Shi, L. Gao and H. Zhu, "Large-scale synthesis of ultralong single-crystalline SiC nanowires," *Phys. Status Solidi A*, vol. 207, no. 11, pp. 2483-2486, 2010.

[102] D. Wei, Y. Shen, M. Li, S. Gao, L. Jia, C. Han and B. Cui, "Synthesis and Characterization of Single-Crystalline SnO2 Nanowires," *J. Nanomater.*, vol. 2013, pp. 1-7, 2013.

[103] S. Vaddiraju, H. Chandrasekaran and M. Sunkara, "Vapor Phase Synthesis of Tungsten Nanowires," *J. Am. Chem. Soc.*, vol. 125, no. 36, pp. 10792-10793, 2003.

[104] C. Ye, X. Fang, Y. Hao, X. Teng and L. Zhang, "Zinc Oxide Nanostructures: Morphology Derivation and Evolution," *J. Phys. Chem. B*, vol. 109, pp. 19758-19765, 2005.

[105] J. Wu, H. Shih and W. Wu, "Formation and photoluminescence of single-crystalline rutile TiO2 nanowires synthesized by thermal evaporation," *Nanotechnology*, vol. 17, no. 1, pp. 105-109, 2005.

[106] S. Lyu, Y. Zheng and C. Lee, "Low-Temperature Growth of ZnO Nanowire Array by a Simple Physical Vapor-Deposition Method," *Chem. Mater.*, vol. 15, pp. 3294-3299, 2003.

[107] L. Wang and X. Zhang, "Synthesis of well-aligned ZnO nanowires by simple physical vapor deposition on c-oriented ZnO thin films without catalysts or additives," *Appl. Phys. Lett.*, vol. 86, no. 2, pp. 024108(1-3), 2005.

[108] L. Brockway, M. Laer, Y. Kang and S. Vaddiraju, "Large-scale synthesis and in situ functionalization of Zn3P2 and Zn4Sb3 nanowire powders," *Phys.Chem. Chem. Phys.*, vol. 15, pp. 6260-6267, 2013.

[109] G. Gundiah, G. V. Madhav, A. Govindaraj, M. Sheikh and C. N. R. Rao, "Synthesis and characterization of silicon carbide, silicon oxynitride and silicon nitride nanowires," *J. Mater. Chem*, vol. 12, p. 1606, 2002.

[110] J. Chen, Q. Shi, L. Xin, Y. Liu, R. Liu and X. Zhu, "A simple catalyst-free route for large-scale synthesis of SiC nanowires," *J. Alloys Compd.*, vol. 509, p. 6844–6847, 2011.

[111] B. Xiang, Y. Zhang, Z. Wang, X. Luo, Y. Zhu, H. Zhang and D. Yu, "Field-emission properties of TiO2 nanowire arrays," *J. Phys. D: Appl. Phys.*, vol. 38, no. 8, pp. 1152-1155, 2005.

[112] Y. C. Kong, D. P. Yu, B. Zhang, W. Fang and S. Q. Feng, "Ultraviolet-emitting ZnO nanowires synthesized by a physical vapor deposition approach," *Appl. Phys. Lett.*, vol. 78, no. 4, pp. 407-409, 2001.

[113] G. Cao, Nanostructures & Nanomaterials: Synthesis, Properties & Applications, London: Imperial College Press, 2004.

[114] M. Fang, N. Han, F. Wang, Z. Yang and J. Ho, "III–V Nanowires: Synthesis, Property Manipulations, and Device Applications," *J. Nanomater.*, vol. 2014, pp. 1-14, 2014.

[115] E. Peled, F. Patolsky, D. Golodnitsky and D. Schneier, "Tissue-like Silicon Nanowires-Based Three-Dimensional Anodes for High-Capacity Lithium Ion Batteries," *Nano Lett.*, vol. 15, pp. 3907-3916, 2015.

[116] M. Adachi, M. Anantram and K. Karim, "Core-shell silicon nanowire solar cells," *Sci. Rep.*, vol. 3, no. 1546, pp. 1-6, 2013.

[117] L. Brockway, V. Vasiraju and S. Vaddiraju, "Compositional disorder and its effect on the thermoelectric performance of Zn3P2 nanowire–copper nanoparticle composites," *Nanotechnology*, vol. 25, no. 12, pp. 125402(1-8), 2014.

[118] R. Wagner and W. Ellis, "Vapor-liquid-solid mechanism of single crystal growth," *Appl. Phys. Lett.*, vol. 4, pp. 89-90, 1964.

[119] A. Morales and C. Lieber, "A Laser Ablation Method for the Synthesis of Crystalline Semiconductor Nanowires," *Science,* vol. 279, pp. 208-211, 1998.

[120] Y. Wu and P. Yang, "Direct Observation of Vapor−Liquid−Solid Nanowire Growth," *J. Am. Chem. Soc,* vol. 123, no. 13, pp. 3165-3166, 2001.

[121] C. Rao, F. Deepak, G. Gundiah and A. Govindaraj, "Inorganic nanowires," *Prog. Solid State Chem.*, vol. 31, pp. 5-147, 2003.

[122] J. Liu, X. Meng, Y. Jiang, C. Lee, I. Bello and S. Lee, "Gallium nitride nanowires doped with silicon," *Appl. Phys. Lett.*, vol. 83, no. 20, pp. 4241-4243, 2003.

[123] D. Banerjee, J. Y. Lao, D. Z. Wang, J. Y. Huang and Z. F. Ren, "Large-quantity free-standing ZnO nanowires," *Appl. Phys. Lett.*, vol. 83, no. 10, pp. 2061-2063, 2003.

[124] M. Khan, X. Wang, K. Bozhilov and C. Ozkan, "Templated Fabrication of InSb Nanowires for Nanoelectronics," *J. Nanomater,* vol. 2008, p. 30, 2008.

[125] C. Schönenberger, C. Schmid, M. Krüger, A. Bachtold, R. Huber, H. Birk and U. Staufer, "Template Synthesis of Nanowires in Porous Polycarbonate Membranes: Electrochemistry and Morphology," *J. Phys. Chem. B,* vol. 101, no. 28, p. 5497–5505, 1997.

[126] W. Han, S. Fan, Q. Li and Y. Hu, "Synthesis of Gallium Nitride Nanorods Through a Carbon Nanotube-Confined Reaction," *Science* , vol. 277, no. 5330, pp. 1287-1289, 1997.

[127] S. Kumar and D. Saini, "Large-scale synthesis of Au-Ni alloy nanowires using electrochemcial deposition," *Appl Nanosci,* vol. 3, no. 2, pp. 101-107, 2013.

[128] T. Gao, G. Meng, Y. Wang and L. Zhang, "Electrochemical synthesis of copper nanowires," *J.Phys:Condens.Matter,* vol. 14, pp. 355-363, 2002.

[129] G. Cao and D. Liu, "Template-based synthesis of nanorod, nanowire, and nanotube arrays," *Adv. Colloid Interface,* vol. 136, pp. 45-64, 2008.

[130] B. Gates, Y. Wu, Y. Yin, P. Yang and Y. Xia, "Single-Crystalline Nanowires of Ag2Se Can Be Synthesized by Templating against Nanowires of Trigonal Se," *J. Am. Chem. Soc,* vol. 123, pp. 11500-11501, 2001.

[131] U. Jeong, P. Camargo, Y. Lee and Y. Xia, "Chemical transformation: a powerful route to metal chalcogenide nanowires," *J. Mater. Chem.*, vol. 16, pp. 3893-3897, 2006.

[132] U. Jeong, Y. Xia and Y. Yin, "Large-scale synthesis of single-crystal CdSe nanowires through a cation-exchange route," *Chem. Phys. Lett.*, vol. 416, pp. 246-250, 2005.

[133] S. Finefrock, H. Fang, H. Yang, H. Darsono and Y. Wu, "Large-scale solution-phase production of Bi2Te3 and PbTe nanowires using Te nanowire templates," *Nanoscale*, vol. 6, p. 7872–7876, 2014.

[134] Y. Kang and S. Vaddiraju, "Solid-State Phase Transformation as a Route for the Simultaneous Synthesis and Welding of Single-Crystalline Mg2Si Nanowires," *Chem. Mater.*, vol. 26, no. 9, p. 2814–2819, 2014.

[135] P. Yang, R. Yan and M. Fardy, "Semiconductor Nanowire: What's Next?," *Nano Lett.*, vol. 10, pp. 1529-1536, 2010.

[136] S. Han, W. Jin and X. Liu, "Controlled growth of gallium nitride single-crystal nanowires using a chemical vapor deposition method," *J. Mater. Res*, vol. 18, no. 2, pp. 245-249, 2003.

[137] M. Zervos, P. Papageorgiou and A. Othonos, "High yield–low temperature growth of indium sulphide nanowires via chemical vapor deposition," *J. Cryst. Growth*, vol. 312, no. 5, pp. 656-661, 2010.

[138] H. Wu, F. Meng, L. Li and G. Zheng, "Dislocation-Driven CdS and CdSe Nanowire growth," *ACS Nano*, vol. 6, no. 5, pp. 4461-4468, 2012.

[139] K. Cho, K. Choi and Y. Kim, "Characterization of GaP nanowires synthesized by chemical vapor deposition," *Material Science Forum*, vol. 534, pp. 25-28, 2007.

[140] S. Panda, J. Sengupta and C. Jacob, "Synthesis of beta-SiC/SiO2 core-sheath nanowires by CVD technique using Ni as catalyst," *J Nanosci Nanotechnol*, vol. 10, no. 5, pp. 3046-3052, 2010 .

[141] D. Stepanchikov and G. Chuiko, "Excitons into one-axis crystals of zinc phosphide," *Condens Matter Phys*, vol. 12, no. 2, pp. 239-248, 2009.

[142] W. Thompson, R. Vaddi and B. White, "Low thermal conductivity in nanocrystalline Zn3P2," *J. Alloys Compd.*, vol. 687, pp. 813-820, 2016.

[143] P. Wu, Y. Dai, Y. Ye, Y. Yin and L. Dai, "Fast-speed and high-gain photodetectors of individual single crystalline Zn3P2 nanowires," *J. Mater. Chem*, vol. 21, pp. 2563-2567, 2011.

[144] L. Brockway, V. Vasiraju, H. Ardakani, R. Yassar and S. Vaddiraju, "Thermoelectric properties of large-scale Zn3P2 nanowire assemblies," *Nanotechnology,* vol. 25, pp. 145401-145408, 2014.

[145] C. Liu, L. Dai, L. You, W. Xu and G. Qin, "Synthesis of high quality p-type Zn3P2 nanowires and their application in MISFETs," *J. Mater. Chem.,* vol. 18, pp. 3912-3914, 2008.

[146] P. Vasekar, D. VanHart and T. Dhakal, "Low-temperature synthesis of Zn3P2 nanowire," *J. Mater. Res,* vol. 26, pp. 1465-1467, 2011.

[147] H. Kamimura, R. C. Gouveia, C. Dalmaschio and A. Chiquito, "Synthesis and electrical characterization of Zn3P2 nanowires," *Semicond. Sci. Technol,* vol. 29, pp. 015001-015005, 2014.

[148] T. Sun, P. Wu, Z. Guo, Y. Dai, H. Meng and L. Dai, "Synthesis and characterization of Zn3P2/ZnS core/shell nanowires," *Phys. Lett. A,* vol. 375, pp. 2118-2121, 2011.

[149] R. Yang, Y. Chueh, J. Morber, R. Snyder, L. Chou and Z. Wang, "Single-Crystalline Branched Zinc Phosphide Nanostructures: Synthesis, Properties, and Optoelectronic Devices," *Nano Lett.,* vol. 7, no. 2, pp. 269-275, 2007.

[150] J. Emsley and P. Udy, "Elucidation of the Reaction of Phosphorus Pentachloride and Ammonium Chloride by Phosphorus-31 Nuclear Magnetic Resonance Spectroscopy," *J. Chem. Soc. A, ,* vol. 0, pp. 3025-3029, 1970.

[151] E. Wiberg and N. Wiberg, Inorganic Chemistry, Academic press, 2001.